Comprehensive Summaries of Uppsala Dissertations
from the Faculty of Science and Technology 631

Electron and Energy Transfer in Supramolecular Complexes Designed for Artificial Photosynthesis

BY

HELENA BERGLUND BAUDIN

ACTA UNIVERSITATIS UPSALIENSIS
UPPSALA 2001

Dissertation for the Degree of Doctor of Philosophy in Physical Chemistry presented at Uppsala University in 2001.

ABSTRACT

Berglund Baudin, H. 2001. Electron and Energy Transfer in Supramolecular Complexes Designed for Artificial Photosynthesis. Acta Universitatis Upsaliensis. *Comprehensive Summaries of Uppsala Dissertations from the Faculty of Science and Technology* 631. 50 pp. Uppsala. ISBN 91-554-5033-4

In the society of today the need for alternative energy sources is increasing. The construction of artificial devices for the conversion of sunlight into electricity or fuel seems very attractive from an environmental point of view, since these devices are based on processes that does not necessarily generate any harmful biproducts. In the oxygen evolving photosynthetic process highly efficient energy and electron transfer reactions are responsible for the conversion of the sunlight into chemically stored energy and if the same principles can be used in an artificial device, the only electron supply required, is water.

This thesis describes energy and electron transfer reactions in supramolecular complexes where the reactions are intended to mimic the basic steps in the photosynthetic process. All complexes are based on ruthenium(II)-trisbipyridine as photosensitizer, that is covalently linked to electron donors or electron or energy acceptors. The photochemical reactions were studied with time resolved transient absorption and emission measurements. In the complexes that mimic the donor side of Photosystem II, where a manganese cluster together with tyrosine catalyses the oxidation of water, intramolecular electron transfer was found to occur from Mn(II) or tyrosine to photo-oxidized Ru(III). Studies of a series of Ru(II)-Mn(II) complexes gave information of the quenching of the Ru(II) excited state by the coordinated Mn(II), which is important for the development of multi-nuclear Ru(II)-Mn complexes. In the supramolecular triad, PTZ-Ru^{2+}-Q, the charge separated state, $PTZ^{+\bullet}$-Ru^{2+}-$Q^{-\bullet}$, was rapidly formed, and further development where a second electron acceptor is linked to quinone is planned. Ultra fast energy transfer (τ<200 fs), was obtained between ruthenium(II) and osmium(II) in a small artificial antenna fragment. Fast and efficient energy transfer is important in larger antennas or photonic wires where a rapid energy transfer is desired over a large distance.

Key words: Artificial photosynthesis, electron transfer, energy transfer, ruthenium, manganese.

Helena Berglund Baudin, Department of Physical Chemistry, Uppsala University, Box 532, S- 751 21 Uppsala, Sweden

ISSN 1104-232X
ISBN 91-554-5033-4

Printed in Sweden by Akademitryck AB, Edsbruk, 2001

List of papers

This thesis is based on the following papers, which will be referred to in the text by their Roman numbers.

I **Intramolecular Electron Transfer from Manganese(II) Coordinatively Linked to a Photogenerated Ru(III)-Polypyridine Complex: A Kinetic Analysis**

H. Berglund Baudin, L. Sun, R. Davidov, M. Sundahl, S. Styring, B. Åkermark, M. Almgren, and L. Hammarström

J. Phys. Chem. A, **1998**, 102, 2512.

II **Mimicking Electron Transfer Reactions in Photosystem II: Synthesis and Photochemical Characterization of a Ruthenium(II) Tris(bipyridyl)Complex with a Covalently Linked Tyrosine**

A. Magnuson, H. Berglund, P. Korall, L. Hammarström, B. Åkermark, S. Styring, and L. Sun

J. Am. Chem. Soc. **1997**, 119, 10720.

III **Ruthenium-Manganese Complexes for Artificial Photosynthesis: Factors Controlling Electron Transfer and Excited State Quenching Reactions**

M. Abrahamsson, H. Berglund Baudin, A. Tran, C. Philouze, K. Berg, M. K. Raymond- Johansson, L. Sun, B. Åkermark, S. Styring, and L. Hammarström

Manuscript to be submitted to Inorg. Chem.

IV **Efficient Light-induced Charge Separation in a Phenothiazine-$Ru(bpy)_3^{2+}$-Quinone Triad**

H. Berglund Baudin, O. Johansson, R. Lomoth, M. Borgström, S. Wallin, L. Sun, B. Åkermark, and L. Hammarström

In manuscript

V **Ultrafast Energy Transfer in Artificial Ruthenium-Osmium Antennas**

H. Berglund Baudin, J. Davidsson, S. Serroni, A. Juris, V. Balzani, S. Campagna, and L. Hammarström

Manuscript to be submitted to J. Phys. Chem.

Comments on my participation

I carry the main responsibility for all experimental work, data analysis and manuscripts in paper I and V. In paper II, I did all photophysical and transient absorption measurements and wrote parts of the manuscript. In paper III, I performed the emission and electron transfer studies in some of the complexes and in paper IV, I was responsible for all femtosecond transient absorption measurements.

Contents

Chapter 1

Introduction

In the photosynthetic process in green plants, algae and cyanobacteria, sunlight is absorbed and converted into chemical energy [1]. The reactions responsible for this process is a series of highly efficient energy and electron transfer steps that results in the formation of energy rich compounds from the reduction of carbondioxide. The electron supply for this process is the oxidation of water that releases oxygen, necessary to sustain life on earth. Since the need for alternative energy sources is increasing in the society of today, much research is devoted to the construction of artificial systems that are capable of absorbing sunlight and convert the energy into electricity or fuel. Systems based on the same principles as in nature are very attractive since the conversion of sunlight into chemically stored energy does not necessarily generate any harmful bi-products, and the only electron source needed is water.

The photosynthetic machinery is located in the thylakoid membrane inside the chloroplasts [1]. The reaction centers Photosystem II (PSII) and Photosystem I (PS I), are large protein complexes positioned in the membrane. To increase the light harvesting efficiency the reaction centers are surrounded by many chlorophyll molecules, capable of absorbing the sunlight, that are arranged in large light harvesting complexes. The structural organization of the chlorophyll pigments within the protein results in an energetically downhill process from the peripheral antenna complexes to the reaction center. The details of the structure and energy transfer process are less well known for oxygen evolving species than in photosynthetic purple bacteria, where the whole process from light absorption to excitation of the reaction center chlorophylls is typically finished within approximately 100 ps [2]. The energy transfer rate between individual pigments within the light harvesting complexes is much faster, and the rate limiting step is believed to be the energy transfer from the core light-harvesting complex I to the reaction center.

In PSII where the oxidation of water occurs, the excitation energy harvested by the antenna complexes eventually leads to excitation of P680, that is the primary electron donor chlorophyll(s) in the reaction center. The excited P680* then

transfers an electron to the acceptor pheophytin and then further to two quinones, Q_A and Q_B. To stabilize the charge separated state the oxidized $P680^+$ is rapidly regenerated by electron transfer from a tyrosyl residue that is positioned between P680 and the manganese cluster that catalyses the oxidation of water [1b,3]. Recent publications have suggested that tyrosine is directly involved in the oxidation of water through a hydrogen atom transfer from a water molecule to the deprotonated tyrosine [4,5]. Four electron transfer cycles eventually leads to oxidation of two water molecules coordinated to the manganese cluster releasing one molecule of oxygen.

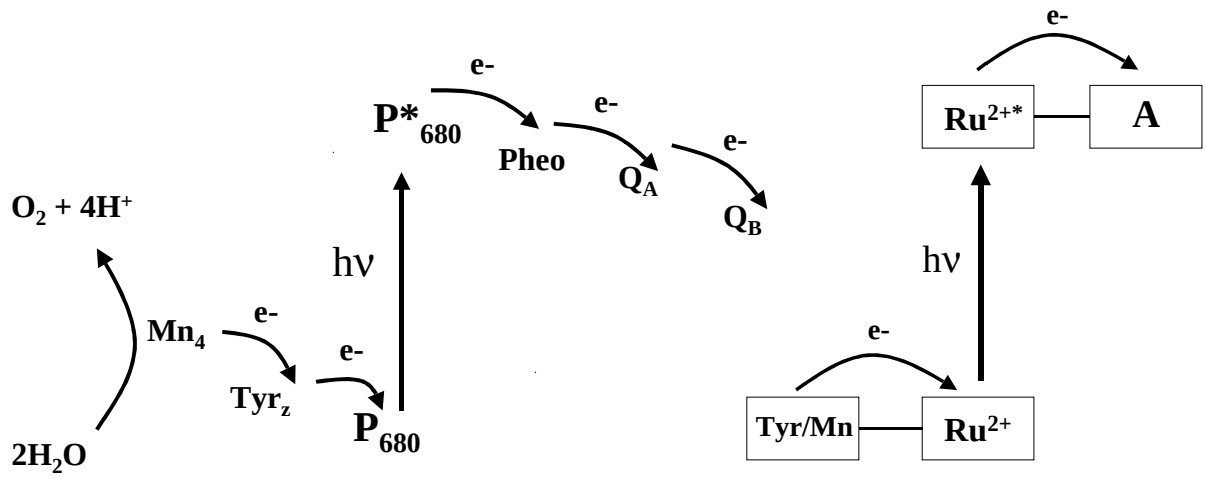

Figure 1.1 Natural (left) versus artificial photosynthesis (right).

Much work is devoted to the understanding of the basic processes of photosynthesis in natural systems and a lot of effort is also devoted to construction of complexes that are able to mimic these processes. Manganese complexes have been constructed as structural mimics of the oxygen evolving center but these have in general not been coupled to light driven reactions [3b,6]. There are several mimics of the primary charge separation process [7,8,9,10,11] but transfer of more than one electron [12] or electron transfer coupled to drive chemical reactions [13] are unusual. Fast and efficient energy transfer over large distances, are interesting for the construction of artificial antennas or photonic wires. Antennas based on porphyrins have been reported where the excitation energy is efficiently transferred to the unit with lowest excited state energy [14,15], recently an artificial antenna have also been coupled to charge separation [16]. Artificial antennas based on transition metal complexes have been constructed where the synthetic procedure allows a control of the exact position of each metal unit [17]. Complexes with as much as 22 metal centers have been synthesized where the absorption in the whole UV

visible range is large [18]. In these complexes the excitation energy is efficiently transferred to the unit with lowest excited state energy [19].

In this thesis, work is presented that concern electron and energy transfer reactions in complexes where the reactions are intended to mimic the basic steps in natural photosynthesis. All complexes are based on $Ru(bpy)_3^{2+}$ as photosensitizer and depending on the nature of the linked compound different reactions involving the $Ru(bpy)_3^{2+}$excited state will occur. In chapter 2 the basic properties of Ru(II)-polypyridine complexes in the ground and excited state are described, and the theories used for electron and energy transfer reactions are briefly presented. Chapter 3 is devoted to electron transfer reactions in complexes that are constructed to mimic the electron transfer reactions on the donor side of PS II. Electron transfer in ruthenium complexes linked with either a tyrosine or manganese ion are presented (Paper I, II, III). The results obtained in these studies where an electron was transferred from tyrosine or Mn(II) to photo-oxidized Ru(III) were the first steps towards mimicking the reactions on the donor side of PS(II), where $P680^+$ is reduced by electron transfer from tyrosine. Factors that govern the electron transfer and the energy wasting, quenching of the excited state of the sensitizer, are discussed. In the last section of chapter 3 some preliminary results on electron transfer in a covalently linked triad are presented, intended for development towards complexes that can be capable of two-electron processes, eventually used for fuel production (Paper IV). The properties of artificial antennas based on transition metal complexes are presented in chapter 4 that also contains results on ultra fast energy transfer in a dinuclear Ru(II)-Os(II) complex (Paper V).

Chapter 2

Photoinduced Processes of $Ru(bpy)_3^{2+}$

Ruthenium(II)-trisbipyridine has been used in numerous investigations as a photosenzitizer during the last 30 years due to the very favorable photochemical properties [20,21].The absorbance in both the visible and UV regions is high. In the excited state, $Ru(bpy)_3^{2+}$ is both a good reductant and oxidant, and the lifetime is long enough to be used in bimolecular electron or energy transfer reactions. In addition both the reduced and oxidized forms are relatively stable towards degrading reactions.

This chapter is intended to give a brief overview of $Ru(bpy)_3^{2+}$ as a photosensitizer. In the first section the properties of the ground and excited states are presented, followed by a description of electron and energy transfer processes involving the excited state, and for a more detailed overview of the properties of $Ru(bpy)_3^{2+}$ there are several review articles and books describing its photophysical and photochemical properties [22,23].

2.1 Properties

2.1.1 The ground state

$Ru(bpy)_3^{2+}$ is a d^6 transition metal complex with octrahedral geometry. A simplified molecular orbital diagram of $Ru(bpy)_3^{2+}$ is shown in Figure 2.1 together with the ground state absorption spectrum. When transition metals like ruthenium form complexes with polypyridine ligands the molecular orbitals created will be localized either predominantly on the metal or on the ligands. Several absorption bands appear in the ground state absorption spectrum that correspond to different types of transitions between the molecular orbitals in the complex. Promotion of an electron from the metal to the ligands is a metal-to-ligand charge transfer (MLCT) transition, whereas promotion of an electron from the ligand to the metal is a ligand-to-metal charge transfer (LMCT) transition. In addition, both metal centered (MC) transitions between orbitals mainly localized on the metal, and ligand centered (LC) transitions between orbitals mainly localized on the ligands, occur. Which transition that will be lowest in energy depends on the oxidation state of the metal and on the nature of

the ligands, but for most Ru(II)-complexes with polypyridine type ligands the transition of lowest energy is the ^{1}MLCT transition [20]. The corresponding lowest excited states are the ^{3}MLCT states.

The ground state electronic configuration of $Ru(bpy)_3^{2+}$ is a singlet state with the six valence electrons in the t_{2g} (π_M) orbitals. When $Ru(bpy)_3^{2+}$ is excited at 450 nm, which is the maximum of the band corresponding to the ^{1}MLCT transition, an electron is transferred to the π^* orbital of the ligands, which is the lowest unoccupied molecular orbital. The ligand centered transitions (LC) of $Ru(bpy)_3^{2+}$, which is transfer of an electron from a π-orbital to π^*-orbital, both localized on the ligand, corresponds to absorption bands in the UV. Metal centered (MC) transitions give rise to a weak absorption band appearing as a shoulder at 350 nm. The LMCT transitions for $Ru(bpy)_3^{2+}$ are high in energy and not visible in the absorption spectrum, but for the oxidized form $Ru(bpy)_3^{3+}$, the LMCT state will be the lowest excited state [21]. In $Os(bpy)_3^{2+}$ the corresponding transitions are at lower energy and due to the enhanced spin-orbit coupling the absorption directly to the triplet states is visible in the spectrum [21].

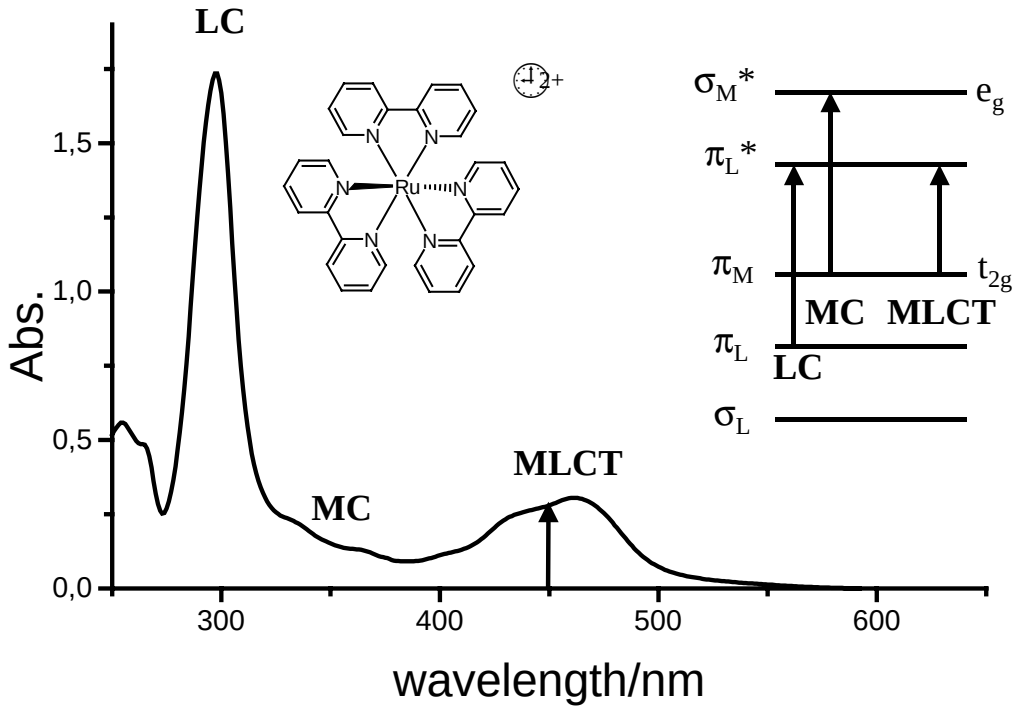

Figure 2.1 Absorption spectrum of $Ru(bpy)_3^{2+}$(in acetonitrile) together with a schematic molecular orbital diagram. For explanations see text.

2.1.2 The excited state

When $Ru(bpy)_3^{2+}$ is excited in the absorption band corresponding to the ^{1}MLCT transition, an electron is promoted from the metal to the ligand(s). The direction of the transition dipole moment for the MLCT transition is along the metal to ligand axis. The excited state is believed to be localized on one bipyridine at a time [24] and the hopping rate between the bipyridine ligands of the excited electron have been reported to occur on the picosecond time scale for $Ru(bpy)_3^{2+}$ in acetonitrile [25,26]. However a recent investigation has indicated that the electron is delocalized over all three ligands initially but that the localization of the electron to one of the bipyridines is ultra fast ($\tau \approx 60$ fs) [27]. The lowest excited state of $Ru(bpy)_3^{2+}$ is the triplet MLCT state and the emission occurs from this state which is believed to consist of three levels which are close in energy [28,29]. Due to the enhanced spin-orbit coupling induced by ruthenium, the conversion from the ^{1}MLCT to ^{3}MLCT is rapid, $\tau \approx 100$ fs [30]. The quantum yield for the formation of the ^{3}MLCT state(s) is near unity [31]. The deactivation of the ^{3}MLCT state is temperature dependent, and at room temperature the lifetime of $Ru(bpy)_3^{2+}$ is 0.6 μs and the quantum yield of emission is 0.04 (water). At 77 K the lifetime is increased to 5 μs and the quantum yield to 0.4 [21].

The lifetime of the ^{3}MLCT state is given by:

$$1/\tau = k_r + k_{nr} + k_{d\text{-}d} \qquad (1)$$

where k_r is the radiative rate constant, k_{nr} is the non radiative rate constant and $k_{d\text{-}d}$ is the rate constant for population of the thermally accessible MC state which decays rapidly to the ground state without radiation. The temperature dependent process is mainly the decay via the thermally activated MC state, which reduces the lifetime of the emission at higher temperatures. The non-radiative rate constant, k_{nr} is dependent on the energy gap between the ground state and the ^{3}MLCT state according to the energy gap law [32]. A smaller energy gap between the lowest excited state and the ground state increases the non radiative rate constant which makes the excited state lifetime shorter. At room temperature the lifetime of $Ru(bpy)_3^{2+}$ is still long enough for the excitation energy to be used in bimolecular photochemical processes.

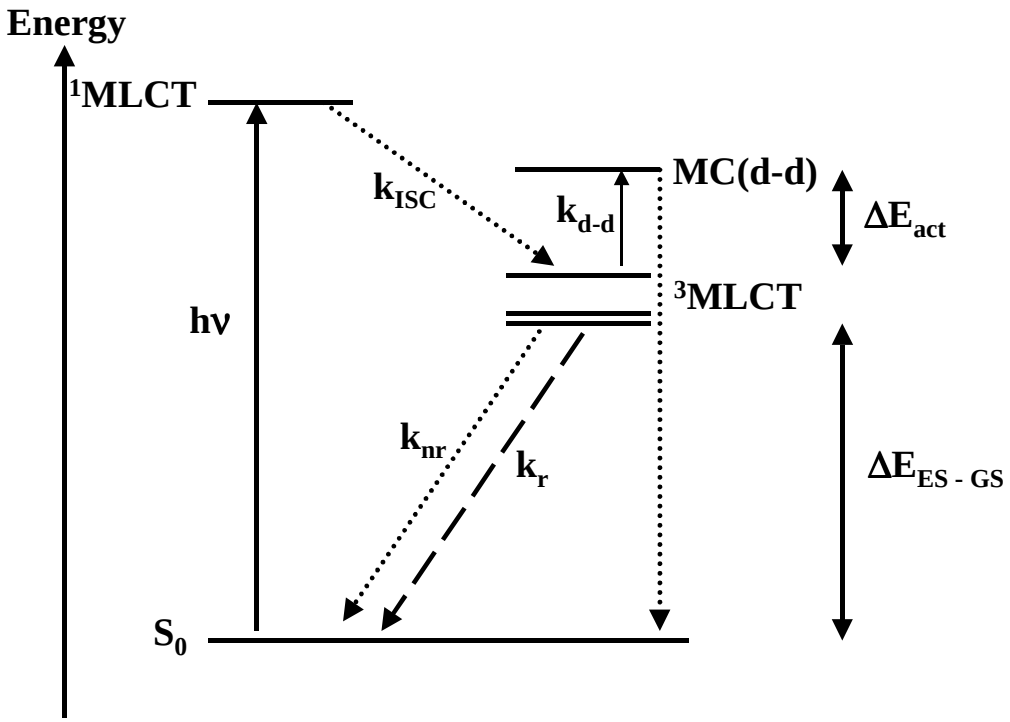

Figure 2.2 Deactivation paths for the excited state. k_{isc} = rate constant for the intersystem crossing from the singlet to triplet state, k_{nr} = rate constant for non radiative decay from the ^{3}MLCT states, k_r = rate constant for radiative decay from the ^{3}MLCT states, ΔE_{act} = activation barrier for population of the MC state, k_{d-d} = rate constant for population of the MC state, $\Delta E_{ES - GS}$ = energy difference between the ground state and ^{3}MLCT states.

The excited state energy of ruthenium polypyridine complexes can be changed by using different ligands [20]. If the same metal coordinates different ligands the lowest MLCT state will be localized on the ligand that is easiest to reduce. It is also possible to fine tune the excited state energy with different substituents on the ligands, that can be either electron donating or withdrawing. This will change the electron density on the ligand and the energy of the MLCT transition will be affected. Investigations have shown that a linear relation exists between the difference of the redox potentials, for the oxidation of the metal and reduction of the ligand, with the energy of the corresponding MLCT transition [33]. This correlation supports a picture where the orbitals involved in the redox-processes are the same as those involved in the charge transfer transitions:

$$E_{MLCT}\,(eV) = E_{ox} - E_{red} + K \qquad (2)$$

where K includes contributions from inner (vibrational) and outer (solvent) reorganization and the difference in Coulombic interaction between the metal and the ligand for the redox states and the MLCT state.

2.2 Excited state reactions

Due to the higher energy content of the excited state, the excited $Ru(bpy)_3^{2+}$ is both a better reductant and oxidant than the ground state. An additional pathway for deactivation of the excited state except the intrinsic decay pathways can be electron or energy transfer to another molecule, where the electron transfer can be either reductive or oxidative.

Oxidative electron transfer	$Ru^{2+}* + Q \rightarrow Ru^{3+} + Q^-$	(3)
Reductive electron transfer	$Ru^{2+}* + Q \rightarrow Ru^{+} + Q^+$	(4)
Energy transfer	$Ru^{2+}* + Q \rightarrow Ru^{2+} + Q*$	(5)

Which mechanism that will dominate depends on the properties of the donor and acceptor. The feasibility of the different deactivation reactions of the excited state can be estimated from the reaction free energy.

In electron transfer reactions the redox potentials of the donor and acceptor ground states can together with the zero-zero excitation energy, $E^{0\text{-}0}$, be used to calculate the redox potentials for the excited state, if the entropy change between the ground state and excited state is assumed to be negligible [20].

$$E^0 (Ru^{3+}/Ru^{2+}*) = E^0 (Ru^{3+}/Ru^{2+}) - E^{0\text{-}0} \quad (6)$$
$$E^0 (Ru^{2+}*/Ru^{+}) = E^0 (Ru^{2+}/Ru^{+}) + E^{0\text{-}0} \quad (7)$$

Then the standard free energy change, ΔG^0, of the reactant and product states, neglecting the coulombic stabilization energy, can be calculated according to:

$$\Delta G^0 = E^0 (Ru^{3+}/Ru^{2+}*) - E^0 (Q^+/Q) \quad (8)$$
$$\Delta G^0 = E^0 (Q^+/Q) - E^0 (Ru^{2+}*/Ru^{+}) \quad (9)$$

If energy transfer is going to contribute as a deactivation path the energy of the excited state of the acceptor must be equal or lower than the energy of the donor excited state. For energy transfer processes the standard free energy change between the reactant and product states can be calculated from the difference of the zero-zero spectroscopic energies, $E^{0\text{-}0}$, of the donor and acceptor excited states according to [34]:

$$\Delta G^0 = E^{0\text{-}0} (A*/A) - E^{0\text{-}0} (D*/D) \quad (10)$$

$E^{0\text{-}0}$ can be calculated from the absorption and emission spectra of the donor and acceptor. If the excited state is a triplet state $E^{0\text{-}0}$ is sometimes estimated from a fit to the emission spectrum [35].

The excited state can be deactivated by the acceptor, Q, in a bimolecular reaction where the donor and acceptor are diffusing in the solution. The quenching rate constant, k_q, is then evaluated according to a reaction scheme which includes the diffusion of the reactants and products. The actual electron or energy transfer step takes place in an encounter complex where the reactants are at short separation distance. In most cases a simplified steady state approximation is valid, giving:

$$k_q = (k_d\, k_e) / (k_{-d} + k_e) \qquad (11)$$

where k_d and k_{-d} are the rate constants for the diffusion of the reactants and k_e is the electron or energy transfer rate constant within the encounter complex. The value of the quenching rate constant can be determined from a Stern-Vollmer relationship. Note however, that the value of k_e can never be directly determined from eq. (11), and that k_q can never exceed k_d, not even for large k_e. An intramolecular reaction between a donor and an acceptor in a preformed complex is not limited by diffusion and can be much more rapid. If the donor and acceptor are connected through bridging units that enhance the electronic coupling electron, and energy transfer (electron exchange) can occur via the orbitals of the bridge (“superexchange”) [36].

2.2.1 Photoinduced electron transfer

In quantum mechanical models the golden rule expression for the transition probability between different electronic states, is often used to treat non adiabatic electron transfer. In the high temperature limit, when the energy of each vibration is considerably less than the thermal energy, $h\nu << k_BT$, the rate constant can be written [37,38]:

$$k_{ET} = (2\pi/\hbar)\, H^2\, (4\pi\lambda k_BT)^{-1/2} \exp(-\Delta G^{\#}/k_BT); \qquad \Delta G^{\#}=(\lambda+\Delta G^0)^2/4\lambda \qquad (12)$$

where H is the matrix element for electronic coupling, λ is the reorganization energy, k_B is the Boltzmann constant, and $\Delta G^{\#}$ is the activation free energy. In the expression for $\Delta G^{\#}$, ΔG^0 is the standard free energy change for the reaction. The rate expression predicts (if the only parameter that is changed is ΔG^0) that the rate of electron transfer will increase with a more negative ΔG^0 until the reaction is activationless, i.e. when $-\Delta G^0$ is equal to the reorganization energy, λ. At this point the rate of electron transfer will be at its maximum. When $-\Delta G^0 > \lambda$

the reaction will be in the inverted region and the rate will decrease again. The reorganization energy λ is the sum of the inner, λ_{in} (vibrational, structural rearrangement within the molecule), and outer, λ_{out} (solvent, rearrangement of the solvent molecules to solvate the new charge situation), reorganization energies. λ_{out} can be estimated from a dielectric continuum model for the solvent, and give the largest contribution to λ in many electron transfer reactions in polar media [38]. λ_{in} can be calculated with knowledge of the reduced force constant, for the vibration involved in the electron transfer reaction, and the equilibrium bond lengths of the reactant and product states [38]. In paper III the temperature dependence of the rate constant for electron transfer between ruthenium and manganese was measured in different Ru(II)-Mn(II) complexes. The resulting value of the total reorganization energy was unusually high which could indicate that large structural rearrangements (inner reorganization) are necessary when Mn(II) is oxidized.

2.2.2 Photoinduced energy transfer

Nonradiative electronic energy transfer between a donor and acceptor in a covalently linked complex can occur if there is some interaction between the two states. This interaction can be divided into two parts, the Coulombic interaction (Förster mechanism) [39,40] and the exchange interaction (Dexter mechanism) [41]. Both mechanisms can act in parallel but due to the nature of the transitions involved and the distance between donor and acceptor, it is often possible to determine which mechanism that is the dominant one.

The Förster mechanism is a through space mechanism based on Coulombic interactions that does not require orbital overlap of donor and acceptor. The Coulombic mechanism is effective when the involved transitions have high oscillator strengths, typically for spin allowed processes such as singlet-singlet energy transfer. This mechanism can occur over distances up to 100 Å. The Dexter mechanism is a short range mechanism, with a distance between donor and acceptor typically shorter than 10 Å, that requires that the orbitals of donor overlap with the orbitals of the acceptor since electrons are exchanged. In contrast to the Förster mechanism, energy transfer according to the Dexter mechanism can occur for spin forbidden processes. The selection rules for the Dexter mechanism requires spin conservation of the reacting pair as a whole. This makes transitions like $D^*(T_1)A(S_0) \rightarrow D(S_0)A^*(T_1)$ allowed. The exchange interaction can be effective over larger distances in linked donor-acceptor molecules, if the connecting bridge allows electronic interactions via the orbitals of the bridge (superexchange, in analogy with electron transfer)

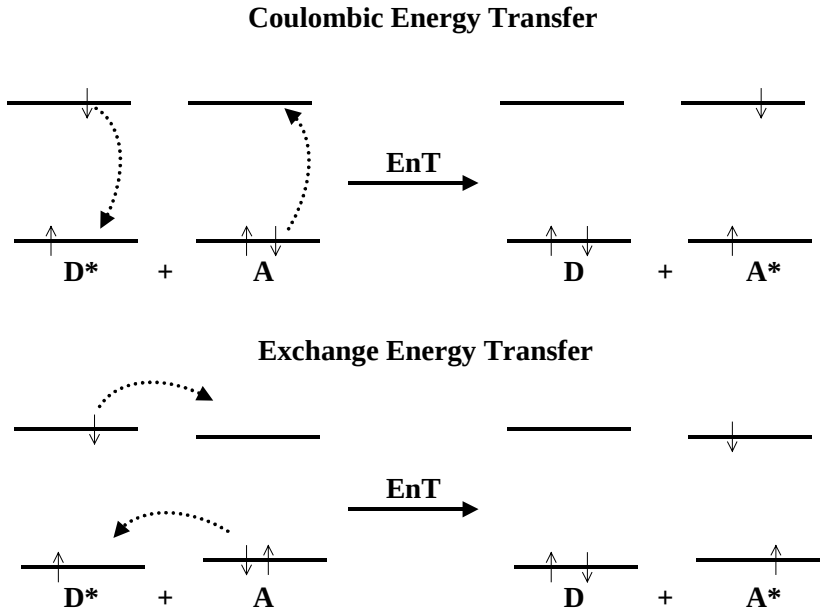

Figure 2.3 Förster and Dexter energy transfer. In the Förster mechanism the dipole-dipole interaction of the donor and acceptor leads to excitation of an electron of the acceptor while the donor is de-excited. The excitation energy is transferred trough space without a need for close contact between the reacting species. In the Dexter mechanism the excited electron on the donor is transferred into the lowest unoccupied orbital of the acceptor with a simultaneous transfer of an electron from the highest occupied orbital of the acceptor to the corresponding orbital of the donor.

A large coupling through the bridge will favor the Dexter mechanism (trough bond) while a more saturated bridge will favor the Förster mechanism (trough space) [42]. The rate constant according to the Förster mechanism can be expressed as [39]:

$$k = \frac{9000(\ln 10)\kappa^2 \phi_D}{128\pi^5 n^4 N_A r^6 \tau_D} J \tag{13}$$

$$J = \int_0^\infty F_D(\nu)\varepsilon_a(\nu)\frac{d\nu}{\nu^4} \tag{14}$$

where ϕ^0_D is the quantum yield of the donor in the absence of acceptor, n is the refractive index of the solvent, N_A is Avogadro´s number, r is the separation distance between donor and acceptor and τ_D is the excited state lifetime of the donor. κ^2 is a factor describing the relative orientation of the transition dipoles for the donor and acceptor respectively. J is the overlap integral that can be calculated from the normalized emission spectrum of the donor and the

absorption spectrum of the acceptor. Thus the rate constant can be calculated from spectroscopic properties of the donor and acceptor.

According to the Dexter (electron exchange) mechanism the rate constant for energy transfer can be expressed as [41]:

$$k = (4\pi^2 / h)\, Z^2\, J' \qquad (15)$$

Where Z is related to the electron matrix element for electron exchange and J′ is the overlap integral. The parameter Z^2 is proportional to exp(-2r/l) where r is the distance between donor and acceptor and l is the sum of the van der Waals radii of the donor and acceptor molecules. Thus, the rate is expected to decrease exponentially with increasing distance between donor and acceptor. The exchange interaction does not depend on the oscillator strengths of the transitions involved in contrast to the Coulombic interaction.

In the non-adiabatic limit the energy transfer according to the electron exchange mechanism can be treated according to the semi-classical expression for electron transfer reactions [43,44]. In the expression for the rate constant (equation 12), the reaction free energy ΔG^0 and the reorganization energy, λ, can be estimated from spectroscopic properties of donor and acceptor respectively, ΔG^0 from the difference of the zero-zero spectroscopic energies and λ from the Stoke´s shift [34]. If ΔG^0 and λ have been estimated the electronic coupling between donor and acceptor can be obtained if the rate constant for the energy transfer process have been measured. In chapter 4 ultra fast energy transfer between Ru(II) and Os(II) at close separation distance is described. The general treatments described in this section are difficult to apply because the ultra fast energy transfer occurs between states that are not thermally relaxed.

2.3 Time resolved studies of electron and energy transfer

Time resolved emission measurements of the excited state lifetime of $Ru(bpy)_3^{2+}$ can give valuable information of the quenching process. For intramolecular processes the rate constant for electron and energy transfer can be obtained by measuring the lifetime of the donor with and without acceptor. In an energy transfer process it can also be possible to measure the rise time of the emission of the acceptor.

If the donors and acceptors that are involved in energy and electron transfer reactions have well known absorption spectra in the different electronic states, transient absorption spectroscopy is a useful technique to monitor the reactions.

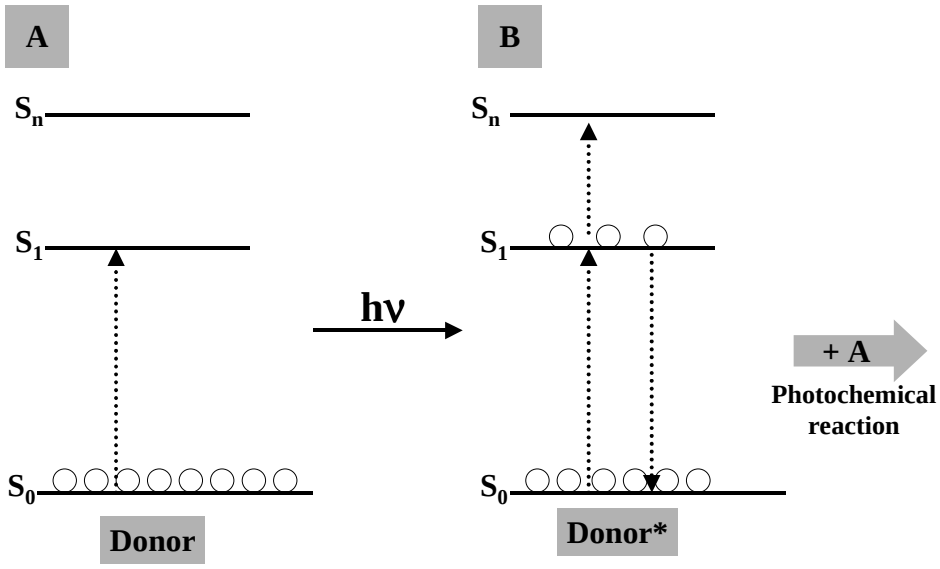

Figure 2.4 A: ground state of the donor molecule, D, B: excited state of D.

In the transient absorbance technique the sample is excited with a laser pulse of a short time duration and then the absorbance is monitored as a function of time. The length of the laser pulse is crucial for what type of reactions that can be studied with a certain laser setup. Short femtosecond laser pulses make it possible to study very fast energy and electron transfer reactions in covalently linked complexes. For slower reactions, like diffusional quenching or the study of triplet absorption, the nanosecond flash photolysis technique is more useful since it provides a longer time window for detection. In this thesis both techniques have been used. In Figure 2.4 a model system (A) is excited with a laser pulse of suitable wavelength to create the excited state of D (B). In the transient absorption spectrum this will be seen as a ground state bleach and excited state absorption. When a photochemical reaction takes place the excited state absorption decays, and the absorption of the products formed in the reaction will appear. If the time window is long enough also the back electron transfer can be studied. At each monitoring wavelength the transient absorption signal will be a sum of the ground state bleach, excited state absorption and the absorption from the species formed in the reaction at different time delays after excitation. If there will be a net bleach or absorption depends on the exctinction coefficients for the species involved in the reaction. If stimulated and spontaneous emission is significant, the contribution to the total signal will appear as a bleaching. A description of the experimental setup used in the nanosecond and femtosecond measurements is given in the Appendix.

Chapter 3

Mimicking the Electron Transfer Reactions of Photosystem (II)

In a Swedish collaboration we have synthesized and studied supra molecular complexes which intend to mimic the donor side of Photosystem II. Several systems have been made based on manganese (II) and tyrosine covalently linked to $Ru(bpy)_3^{2+}$ [45,46,47,48,49]. The aim was to investigate the possibility of electron transfer from Mn(II) or tyrosine to photo-oxidized Ru(III) after quenching of the excited Ru(II)* by an external electron acceptor. More sophisticated systems have also been made where Ru(II) is linked with a tyrosine and two Mn (II) ions [50].

In this chapter the first results which was obtained on intramolecular electron transfer from a covalently linked Mn(II) or tyrosine to photo-oxidized Ru(III) will be presented (Paper I and II, III]. Other processes that may complicate the electron transfer as quenching of the excited state of Ru(II)* by the linked Mn(II) and dissociation of Mn(II) from the Ru(II)–Mn(II) complex will be discussed. In the last section some preliminary results of electron transfer in a covalently linked triad, will be presented.

3.1 Electron transfer from Mn(II) linked to photo-oxidized Ru(III)

3.1.1 Quenching of the excited state of ruthenium by Mn(II)

For efficient electron transfer to an external acceptor the lifetime of the excited state is of crucial importance. If the lifetime is too short the excited state will decay to the ground state before any photochemical reaction has time to occur. The lowest excited state of $Ru(bpy)_3^{2+}$ is the ^{3}MLCT state and the lifetime in acetonitrile at room temperature is ≈900 ns, which is enough for a diffusion controlled reaction with an acceptor. Without coordinated Mn(II) the lifetime of the complexes shown in Figure 3.1 is 980, 1050, and ≈900 ns respectively, which is approximately the same as for $Ru(bpy)_3^{2+}$. However when Mn(II) is coordinated the lifetimes decrease to 250, 7, and ≈300 ns respectively. The desired reaction for the Ru(II)-Mn(II) complexes is intramolecular electron

transfer from the coordinated Mn(II) to photo-oxidized Ru(III) and not a competing process that quenches the excited state of ruthenium before an electron is transferred to the external acceptor. Therefore it is important to make the quenching of the excited state of Ru(II) as slow as possible but at the same time the electron transfer from Mn(II) to Ru(III) should be fast and efficient.

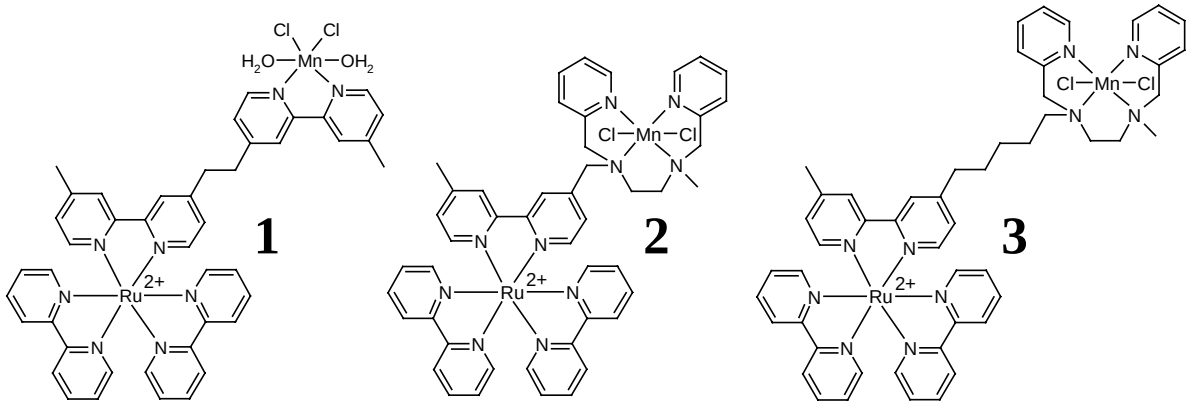

Figure 3.1 Structure of the Ru(II)-Mn(II) complexes. The metal-to-metal distance is 13, 9 and 14 Å respectively, estimated from simple molecular modeling.

Different reasons for the shorter lifetime of the MLCT state of $Ru(bpy)_3^{2+}$ can be considered. If the electronic structure of ruthenium is changed when Mn(II) is coordinated, the energy of the MLCT state can be changed which will affect the intrinsic deactivation rate constants. Due to the small variation of the absorption and emission spectra compared to the complexes without Mn(II) this is not believed to be the explanation for the shorter lifetimes in the Ru(II)-Mn(II) complexes. The quenching is therefore attributed to a new deactivation mechanism in the presence of coordinated Mn(II).

Different mechanisms are conceivable; A. Electron transfer from Mn(II) to excited Ru(II)* generating Mn(III) and Ru(I). B. Energy transfer to an excited state of Mn(II) from the excited Ru(II) generating Mn(II)* and Ru(II). C. A third possibility is paramagnetic quenching which for ruthenium complexes is believed to be of no significance [51]. To get a better understanding for the quenching process, low temperature emission lifetime measurements were performed on **1** (Paper I) as well as on a number of other Ru(II)-Mn(II) complexes (Paper III). The results indicated that the quenching occurred by energy transfer and not electron transfer. Approximately the same lifetime of the intact Ru(II)-Mn(II) complexes was obtained at 77 K as at room temperature, indicating that the reaction free energy, ΔG^0, for electron transfer was not significantly decreased at lower temperature. For quenching via electron transfer a decrease of the driving force is expected at low temperature since the solvent

cannot reorganize in response to the new charge distribution. Thus, ΔG^0 would increase by an amount equal to the reorganization energy which would be c. a. 1.0 eV [52,53,54]. Since the calculated driving force was close to zero already at room temperature, electron transfer quenching would be strongly endothermic at 77 K. For energy transfer the outer reorganization is much smaller than for electron transfer and thus the temperature difference would have a smaller effect on the quenching rate, consistent with our observations. Förster-type energy transfer can be ruled out by the very weak absorption of Mn(II)-complexes in the visible region, since the transitions in Mn(II) are both symmetry and spin forbidden. However energy transfer via the Dexter mechanism may be spin-allowed for energy transfer from the ^{3}MLCT state of Ru(II). The quenching rate constant was found to decrease exponentially with increasing distance between Ru(II) and Mn(II) (Paper III) and this is consistent with energy transfer via an exchange mechanism. The conclusion drawn is that in order avoid a too fast quenching of the excited state of Ru(II)* the distance between the coordinated Mn(II) and Ru(II) should be kept long enough. Unfortunately this is probably in conflict with fast and efficient electron transfer after photo-oxidation of Ru(II).

One possible solution to this problem was to introduce tyrosine as a redox intermediate between Mn(II) and Ru(II). Emission and transient absorption measurements showed that tyrosine did not quench the excited state of ruthenium compared to a model compound, and after oxidation of ruthenium tyrosine was also capable of transferring an electron to Ru(III) regenerating Ru(II). In PS II, TyrosineZ is positioned between P680 and the manganese cluster functioning as a redox intermediate [1b,4]. Maybe this is nature´s solution to avoid quenching of P680* before the desired electron transfer reactions occur. In section 3.2 the results on electron transfer studies from tyrosine to photo-oxidized Ru(III) will be presented.

It has also been shown in paper III that strong electron withdrawing groups on the Ru(II)-ligands that are remote from the Mn(II)-moiety make the quenching of the excited state much slower, while the electron transfer rate from Mn(II) to Ru(III) is even somewhat higher. Since the lowest MLCT state will then be localized on the ligand easiest to reduce [20], electron withdrawing groups on the bipyridines results in localization of the electron to those ligands which in this case will increase the effective distance between the Ru(II) excited state and Mn(II).

3.1.2. Electron transfer from Mn(II) to photo-oxidized Ru(III)

The first successful intramolecular electron transfer from Mn(II) to Ru(III) was obtained in complex **1** (Paper I). At this time it was still unknown if

intramolecular electron transfer was going to occur. From the redox potentials of $Mn^{II/III}$ (0.9 V) and $Ru^{II/III}$ (1.3 V) (vs SCE in CH_3CN), the driving force for electron transfer was calculated to be 0.4 eV. Thus it seemed thermodynamically feasible to reduce Ru(III) by the coordinated Mn(II). Transient absorption measurements showed that after the competing Ru(II)* quenching processes by Mn(II) and the external electron acceptor, MV^{2+}, the charge separated state was formed creating Ru(III) and the reduced acceptor $MV^{+\bullet}$ in equimolar concentrations[55,56,57]. The ground state bleach of Ru(II) due to formation of Ru(III) was monitored at 450 nm. The formation and decay of the reduced acceptor was monitored at 600 nm where $MV^{+\bullet}$ is known to absorb. The oxidation of Mn(II) could not be observed in the transient absorption measurements due to the very weak absorption of both Mn(II) and Mn(III).

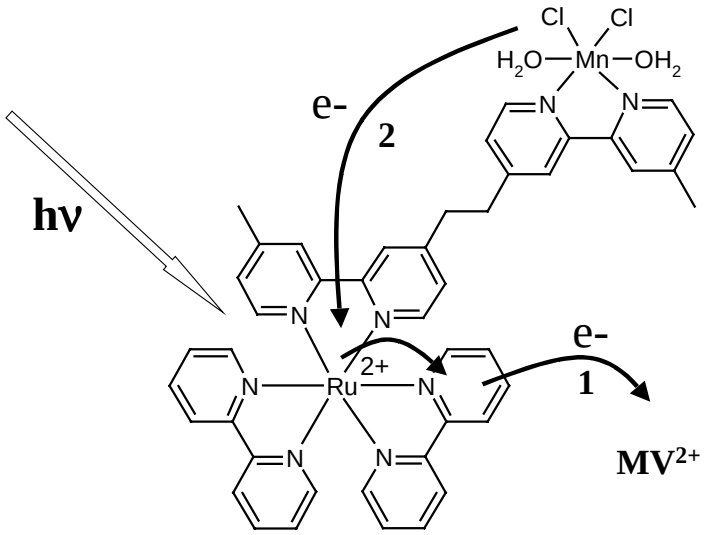

Figure 3.2 1: Electron transfer from the excited state of Ru(II)* to MV^{2+}. 2: Intramolecular electron transfer from Mn(II) to Ru(III).

In the model compound the recovery at 450 nm and the decay at 600 nm occurred with the same second order rate constant, attributed to recombination between Ru(III) and $MV^{+\bullet}$. In Ru(II)-Mn(II) the decay of $MV^{+\bullet}$ occurred with the same second order rate constant as for the model compound without coordinated Mn(II). However the recovery of Ru(II) observed at 450 nm was much faster. The ligand was not a possible electron donor on the observed timescale that was shown in the measurements with the model compound. The only source present except $MV^{+\bullet}$ capable of giving an electron to oxidized ruthenium was then Mn(II). Since the electron did not come from $MV^{+\bullet}$ the conclusion was that it must have come from Mn(II). Thus the desired electron transfer from Mn(II) to photo-oxidized Ru(III) occurred.

The electron transfer between Mn(II) and Ru(III) was also confirmed by EPR measurements where chemically produced $Ru(bpy)_3^{3+}$ was mixed with an equimolar amount of complex **1**, which contains Mn(II). Ru(III) and Mn(II) show characteristic EPR signals whereas Ru(II) and Mn(III) are EPR silent. The signals disappeared after mixing which showed that Ru(III) was capable of oxidizing Mn(II) [46].

However a dependence of the rate constant on the concentration of the Ru(II)-Mn(II) complex was observed and the kinetic traces were not simple single exponentials. This is not expected for an intramolecular electron transfer reaction. Thanks to the Ru(II)* quenching process, steady state and time resolved emission measurements could show that Mn(II) dissociated from the complex leaving one fraction without bound Mn(II) in the solution. These fractions could be quantified from a biexponential fit of the emission decay. A kinetic model was assumed were intramolecular electron transfer occurred in the intact complex, $Ru^{III}LMn^{II}$, and in the complexes without bound manganese, $Ru^{III}L$, electron transfer could only occur after reassociation of Mn(II). In Figure 3.3 the reaction scheme for the processes included in the kinetic model is shown.

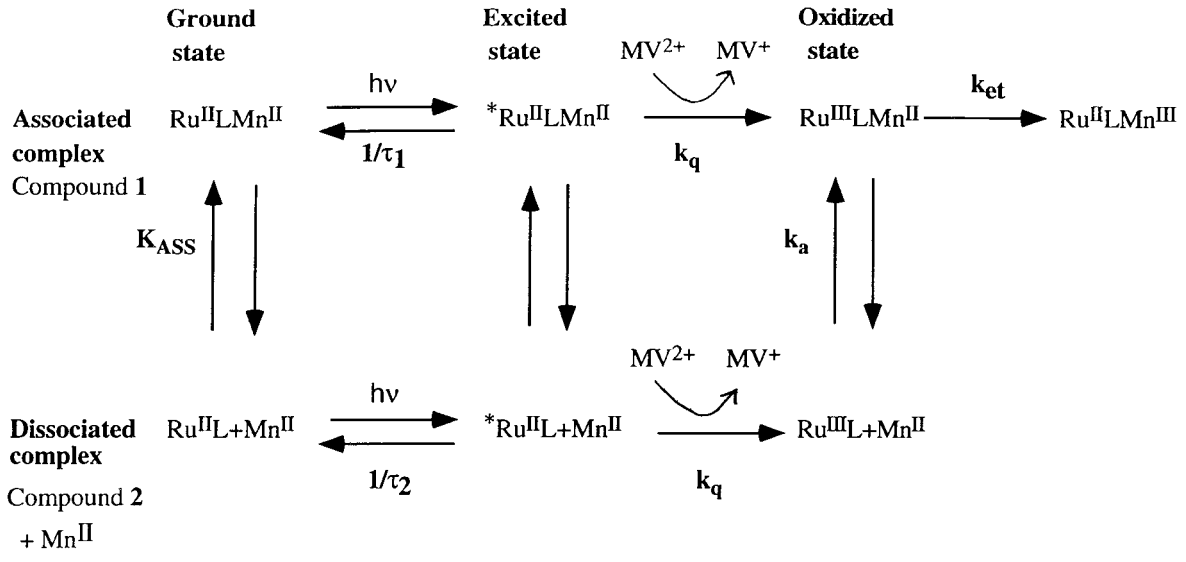

Figure 3.3 Reaction scheme for the electron transfer processes included in the kinetic analysis of the recovery of Ru(II) at 450 nm.

The disappearance of Ru(III) was observed as a recovery of the bleach at 452 nm after the decay of the excited state. The disappearance of the total concentration of Ru(III) after the decay of the excited state is given by:

$$\left(\left[Ru^{III}LMn^{II}\right]+\left[Ru^{III}L\right]\right)(t)=\left(\left[Ru^{III}LMn^{II}\right]_0-\frac{k_a\left[Mn^{II}\right]\left[Ru^{III}L\right]_0}{k_{et}-k_a\left[Mn^{II}\right]}\right)\frac{e^{-k_{et}t}}{k_{rec}\left[MV^{+}\right]_0 t+1}+ \quad (16)$$

$$+\frac{k_{et}\left[Ru^{III}L\right]_0}{k_{et}-k_a\left[Mn^{II}\right]}\frac{e^{-k_a[MnII]\,t}}{k_{rec}\left[MV^{+}\right]_0 t+1}$$

The parameters k_{et} and $k_a[Mn^{II}]$ and the total concentration of Ru(III) ($[Ru^{III}]_0$tot = $[Ru^{III}LMn^{II}]_0$ + $[Ru^{III}L]_0$) initially formed, were determined from a fit of the kinetic traces to equation 16 at each total concentration of complex **1**. The initial fractions of $[Ru^{III}LMn^{II}]_0$ and $[Ru^{III}L]_0$ and the value of $k_{rec}[MV^{+}]_0$ were fixed in the fitting procedure and determined in independent experiments. The resulting values of k_{et} and $k_a[Mn^{II}]$ from the curve fit were plotted versus the concentration of free Mn(II). As can be seen in Figure 3.4, k_{et} is constant with increasing concentration of free Mn(II) whereas $k_a[Mn^{II}]$ shows the expected linear concentration dependence. This was assumed in the kinetic model and the results obtained were consistent with that. The rate constant for intramolecular electron transfer from Mn(II) to Ru(III) was obtained as $k_{et}=1.8\times10^5$ s^{-1} and the rate constant for association of Mn(II) with the dissociated complex was obtained as 2.9×10^9 $M^{-1}s^{-1}$.

Control experiments were needed for further support of the kinetic model, that is not unique. *Inter*molecular electron transfer from Mn(II) to photogenerated Ru(III) on different complexes could also be an explanation for the concentration dependent process. However stopped-flow experiments, in which chemically produced Ru(III)$(bpy)_3$ was mixed with complex **1** and the disappearance of Ru(III) was monitored optically, ruled out this explanation. The obtained rate constant for the bimolecular process was too slow ($\approx1\times10^6$ $M^{-1}s^{-1}$), to explain the observed concentration dependence in Figure 3.4 Electron transfer from dissociated Mn(II), free in solution was excluded based on experiments where $Ru(bpy)_3^{2+}$ was titrated with $MnCl_2$ and the emission of $Ru(bpy)_3^{2+}$ was measured.

Intramolecular electron transfer also occurred in complexes **2** and **3**, with rate constants $k_{et}>2\times10^7$ s^{-1} and $k_{et}\approx1\times10^5$ s^{-1} respectively. The short lifetime of the excited state of **2** required a very high concentration of the external acceptor, MV^{2+}, to compete with intramolecular quenching of the excited state of Ru(II)*

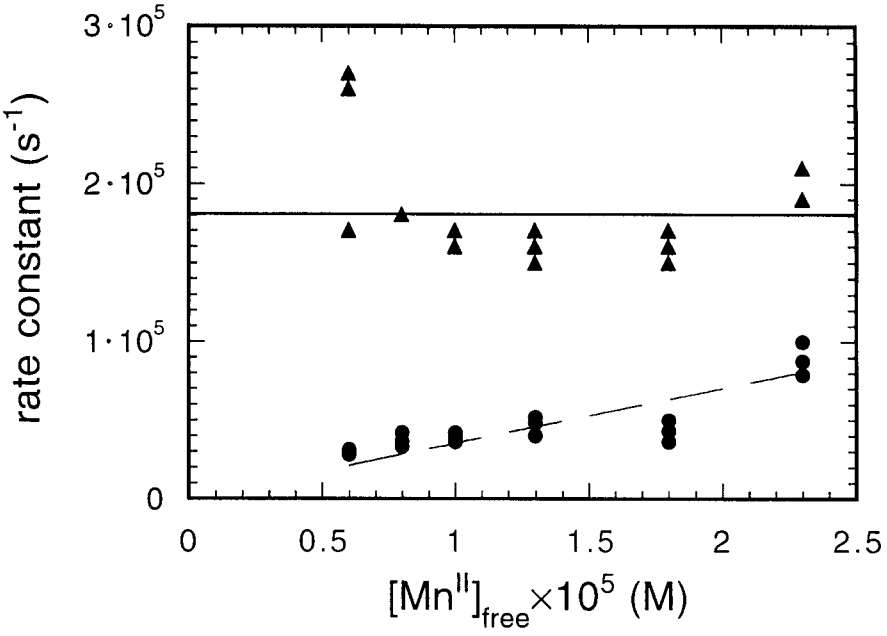

Figure 3.4 Rate constant for intra molecular electron transfer, k_{et} versus the concentration of free Mn(II) (triangles) and psedo-first order rate constant, $k_a[Mn^{II}]_{free}$ versus free Mn(II) (circles).

by Mn(II). The dissociation of Mn(II) in complexes **2** and **3** was less significant than for complex **1** and a simpler kinetic analysis could be applied.

Temperature dependent measurements of the electron transfer rate in different Ru(II)-Mn(II) complexes (Paper III) have shown that the inner reorganization energy is unusually high in these complexes. This is probably due to a large reorganization of the coordination site when Mn(II) is oxidized to Mn(III). This could indicate that this type of manganese complexes never will be fast electron donors. This was another reason –except to avoid fast quenching of the excited state of Ru(II)*– for introducing a redox intermediate such as tyrosine between ruthenium and manganese. Then tyrosine could act as a fast electron donor to regenerate Ru(II). A third reason for introducing an intermediate electron donor is to avoid *reduction* of higher oxidation states of the manganese complex by the excited Ru(II)*. This will be important in multistep oxidation of the manganese complex where the intention is oxidation of water. Our first attempt of electron transfer from tyrosine to photo-oxidized ruthenium will be presented in the next section.

3.2 Electron transfer from tyrosine to photo-oxidized Ru(III)

In the last section, three reasons for introduction of an intermediate electron donor between Ru(II) and Mn(II) was mentioned that are of particular interest

for avoiding unwanted reactions of the Ru(II)* excited state. In addition, it also seemed interesting to use tyrosine as an electron donor to further mimic the reactions of PS II.

A complex was synthesized where ruthenium was covalently linked to a tyrosine residue via an amide bridge (Figure 3.5). Time resolved emission measurements showed that the excited state decay was not affected by the linked tyrosine. The lifetime in water solution at pH=7 was 370 ns, the same as for the model compound where ruthenium was linked to an alanine. The redox potential of tyrosine is +0.97 V in water at pH=7 [47]. This makes electron transfer to Ru(III) thermodynamically feasible, $\Delta G^0 = -0.3$ eV. Transient absorption and EPR measurements were used to investigate the intramolecular electron transfer reaction.

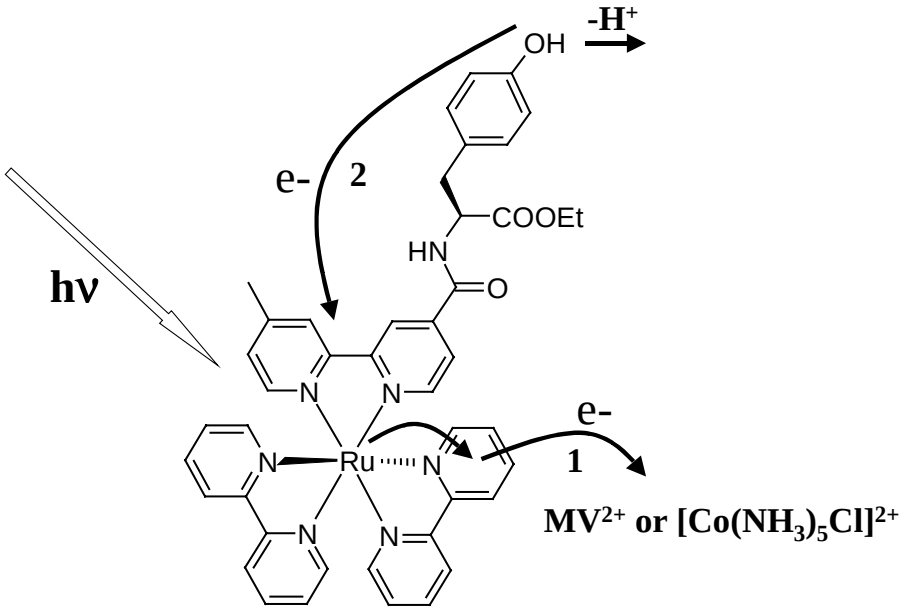

Figure 3.5 1: Electron transfer from excited Ru(II)* to MV^{2+} or Co^{3+}. 2: Intramolecular electron transfer from tyrosin to Ru(III) with a simultaneous deprotonation [48].

Excitation of the Ru(II)-moiety of the Ru(II)-Tyr complex in the presence of the external acceptor MV^{2+} resulted in charge separation. The appearance and decay of $MV^{+\bullet}$ was monitored at 600 nm and the bleaching and recovery of Ru(II) was monitored at 450 nm. After the quenching of Ru(II)* by MV^{2+} was completed, the decay of the oxidized Ru(III) and reduced $MV^{+\bullet}$ was followed kinetically. The recovery of Ru(II) occurred with a rate constant of $k= 5 \times 10^4$ s^{-1}, while the decay of the absorbance signal from $MV^{+\bullet}$ was much slower. The conclusion was that intramolecular electron transfer from tyrosine occurred regenerating Ru(II). For the model compound (without tyrosine) it was found that the decay

of $MV^{+\bullet}$ and recovery of Ru(II) occurred with the same second order rate constant ($k=8 \times 10^9$ $M^{-1}s^{-1}$) consistent with a diffusion controlled recombination between MV^+ and Ru(III). Further support that Ru(II) was regenerated by the tyrosine moiety was obtained when a sacrificial electron acceptor, $Co(NH_3)_5Cl^{2+}$, was used that also give negligible transient absorption changes in the near UV-vis region upon reduction.

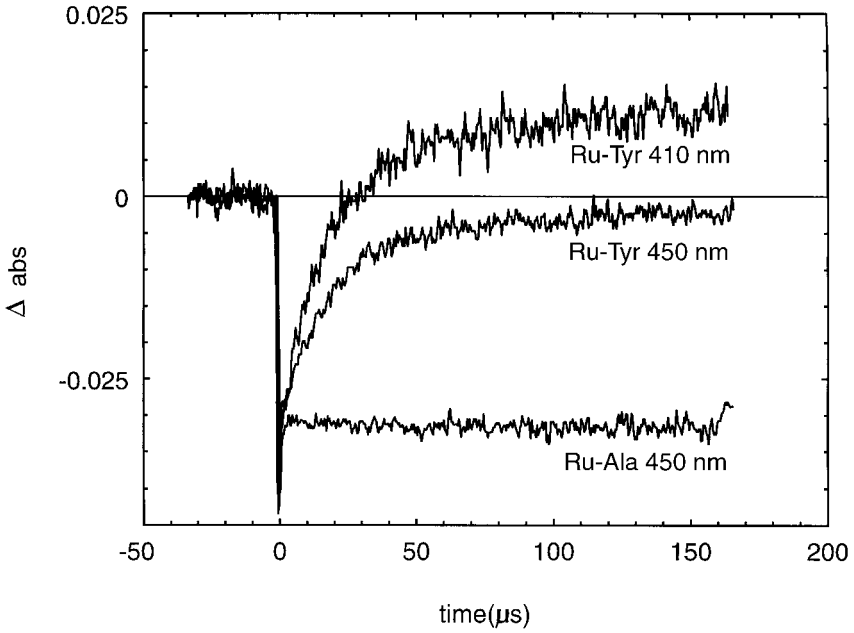

Figure 3.6 Kinetic traces at 450 and 410 nm for Ru-Tyr and Ru-Ala, with $Co(NH_3)_5Cl^{2+}$ as electron acceptor. The increased absorption at 410 nm was attributed to absorption from the tyrosine radical, formed in the electron transfer reaction with Ru(III). For the model compound Ru-Ala, recovery of Ru(II) was not observed on the measured time scale.

At 410 nm, where tyrosine radicals has been reported to absorb [58] an absorption appeared, after the recovery of the initial bleaching. This was attributed to absorption from the oxidized tyrosine. The recovery of the 450 nm signal for the Ru(II)-Tyr complex occurred with the same rate as when MV^{2+} was used, whereas the signal at 450 nm for the model compound did not decay at all in the observed time window. To rule out the possibility of intermolecular electron transfer between Ru(III) and tyrosine on different complexes, a control experiment was performed where a solution of $Ru(bpy)_3^{2+}$, MV^{2+} and free tyrosine was flashed. However, the rate constant for the bimolecular reaction was two orders of magnitude too small to account for the rate obtained in the experiments with the Ru(II)-Tyr complex.

EPR measurements confirmed that a light-induced oxidation of the tyrosine moiety occurred. Important information was also obtained on the lifetime of the oxidized tyrosine radical, which could not be followed in the transient

absorption measurements at 410 nm. An EPR spectrum was recorded of the Ru(II)-Tyr complex during illumination in the presence of the sacrificial acceptor $Co(NH_3)_5Cl^{2+}$. An EPR signal centered around g=2.0044 was obtained and attributed to the oxidized tyrosine residue, due to the high g-value that is very similar to the g-values of other neutral tyrosyl radicals [59,60] The second order decay of the radical was measured by time resolved EPR and the first half-life was found to be 50 ms. Intramolecular electron transfer from a phenol type ligand to a photo-oxidized Ru(II)-complex has also recently been reported by Wieghardt et al.[61,62].

In a later publication it has been shown that the Ru(II)-Tyr complex was capable of oxidizing a manganese (III/III) dimer [47]. Other interesting results have also been obtained concerning the pH-dependence of the electron transfer rate in the Ru(II)-Tyr complex [48]. The fact that intramolecular electron transfer occurred in the Ru(II)-Tyr complex, and the following investigations were each a step further, towards mimicking the reactions in PS II. A complex where Ru(II) is linked to a Mn(II/II) dimer via a tyrosine residue has been prepared in which intra molecular electron transfer from the Mn(II/II) dimer to the photo-oxidized Ru(III) occurred with a rate constant larger than 1×10^7 s^{-1} (limited by the quenching of the excited state by the external acceptor) [50]. To be able to resolve the electron transfer from the manganese dimer a faster acceptor has to be used. A covalently linked electron acceptor might solve this problem. To ultimately achieve the goal of water oxidation higher oxidizing states of the manganese complex have to be used, and work is in progress with modified ligands to stabilize higher valence states of the Mn-dimer. For a recent review on the results so far on the Mn_2-Tyr-Ru(II) complexes intended to mimic the donor side of PS II see reference [63].

3.3 Electron transfer in a covalently linked triad

To eventually be able to produce H_2 at a catalytic metal center, the development of artificial models of the acceptor side of PS II is very interesting. In addition faster electron acceptors are needed to be able to oxidize Ru(II), when the quenching of the Ru(II) excited state by Mn(II) is too rapid, and to resolve the intramolecular electron transfer from Mn(II) to photo-oxidized Ru(III).

In order to develop a complex where the electron can be transferred to a second acceptor (Figure 3.7), the competing back electron transfer from the primary acceptor to the oxidized photo-sensitizer must not be too fast. Charge separation in a covalently linked Ru(II)-MV^{2+} donor acceptor complex and the corresponding back electron transfer had been reported to occur rapidly, with a

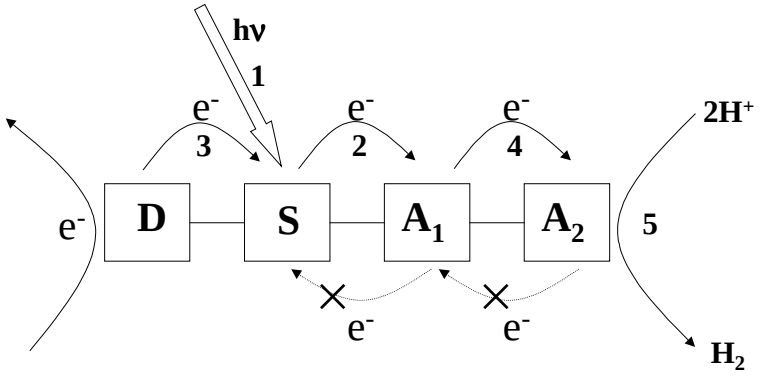

Figure 3.7 Schematic picture of a donor-acceptor system for hydrogen evolution. 1: Excitation of the photosensitizer, 2: electron transfer to the primary acceptor, 3: fast electron donation to stabilize the charge separated state, 4: electron transfer to a second electron acceptor which after a second cycle can be double reduced, 5: the electrons are used to produce H_2.

time constant for the back reaction of ≈25 ps [64]. To increase the probability of avoiding the back reaction, MV^{2+} was exchanged for quinone since the forward and backward electron transfer steps had been reported to be slower [65]. Another reason for using quinone as electron acceptor is their capability to accept two electrons, which is interesting for the reduction of $2H^+$ to H_2.

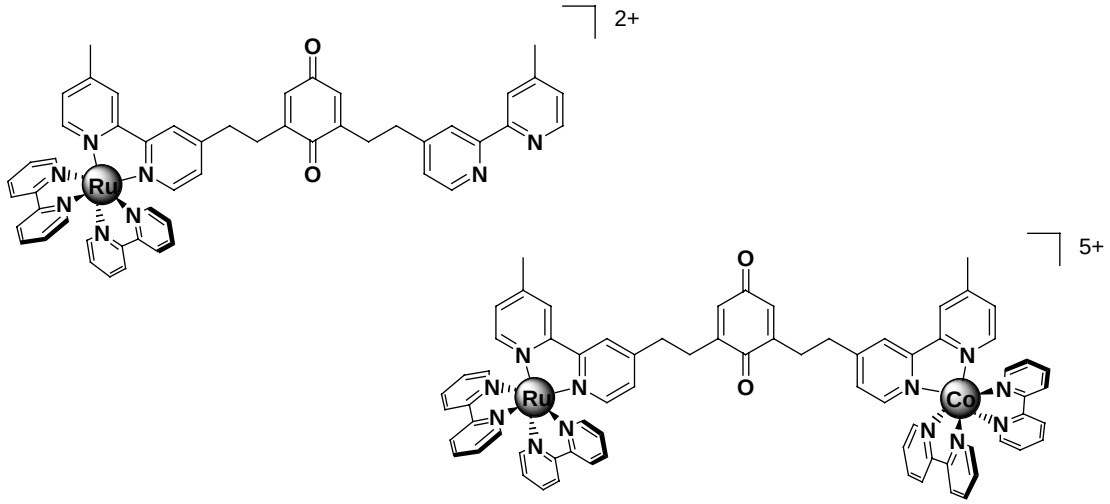

Figure 3.8 Ru^{2+}–Q (left) and Ru^{2+}–Q–Co^{3+} (right).

Two complexes were made Ru^{2+}–Q and Ru^{2+}–Q–Co^{3+}, where a second electron transfer step from $Q^{-\bullet}$ to Co^{3+} was expected to be thermodynamically feasible from redox data [66]. Femtosecond transient absorption measurements showed that, the forward and backward electron transfer reactions in the Ru^{2+}-Q complex occurred with a ≈200 ps and ≈900 ps time constant, respectively.

However in the Ru^{2+}–Q–Co^{3+} complex the back electron transfer from $Q^{-\bullet}$ to Ru(III) ($\tau \approx 900$ ps) dominated. To solve this problem and be able to eventually succeed in a second electron transfer step, another compound was synthesized where the electron donor phenothiazine (PTZ) was covalently linked to the Ru^{2+}-Q complex (Figure 3.9). PTZ has been reported to be a fast electron donor to Ru(III) in the covalently linked triads PTZ-Ru^{2+}-AQ (phenothiazine-ruthenium-anthraquinone) [67], PTZ-Ru^{2+}-MV^{2+} [68] and in PTZ-Ru^{2+}-DQ^{2+} [69]. If PTZ could work as a fast electron donor to Ru(III) in our system the charge separated state would be stabilized and the back reaction from quinone to Ru(III) prevented. This would increase the possibility of a second electron transfer step to a second acceptor. The corresponding dyad PTZ-Ru^{2+} was also synthesized as a model compound.

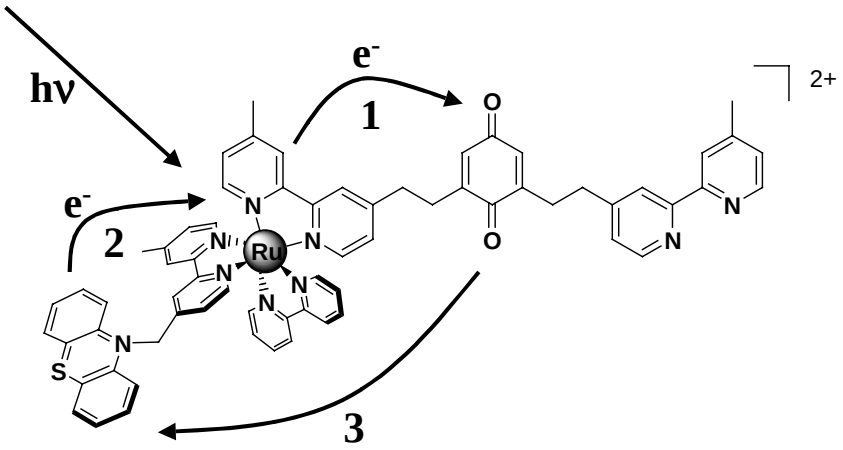

Figure 3.9 The PTZ-Ru^{2+}-Q triad with electron transfer reactions. 1: Electron transfer from excited Ru(II) to quinone, 2: fast electron donation from PTZ to Ru(III). 3: Back electron transfer from reduced quinone to oxidized phenothiazine.

Preliminary results from femtosecond transient absorption measurements showed that the charge separated state, $PTZ^{+\bullet}$–Ru^{2+}–$Q^{-\bullet}$ was formed with a time constant of ≈200 ps, that is approximately the same as the electron transfer lifetime in Ru^{2+}–Q. This suggests that the initial electron transfer from Ru(II)* is rate limiting ($\tau \approx 200$ ps), and that the subsequent PTZ-to-Ru(III) electron transfer is much faster. An absorption appeared at 510 nm, where $PTZ^{+\bullet}$ is known to absorb [67], with the same rate as the decay at 450 nm. Measurements of the model compound PTZ-Ru(II) showed that the excited Ru^{2+}* was quenched only slowly by PTZ, giving an emission lifetime of 90 ns in degassed acetonitrile.

A full spectrum was taken with nanosecond flash photolysis to identify the spectral features of the charge separated state and then measure the rate of the

back reaction. The reduced quinone was not observed in the femtosecond transient absorption measurements, probably due the presence of Ru^{2+}*, of which the bleaching cancelled the $Q^{-\bullet}$ absorption. However, with the help of a control experiment where $Ru(bpy)_3^{2+}$ was mixed with bensoquinone and a spectra of the charge separated state was taken, absorption bands corresponding to the reduced quinone could be identified in the flash photolysis spectrum of the triad. The back electron transfer:

$$PTZ^{+\bullet}–Ru^{2+}–Q^{-\bullet} \rightarrow PTZ–Ru^{2+}–Q \qquad (17)$$

was found to occur with a time constant of 90 ns, approximately the same as for the back electron transfer reported for PTZ-Ru^{2+}-AQ [67].

In the femtosecond experiments with PTZ-Ru^{2+}-Q the results indicated that a fraction of Ru^{2+}* was not involved in the electron transfer to Q. This was further confirmed in nanosecond emission measurements where a rather large emission signal was observed at 600 nm, where Ru(II) have emission. This could be attributed to photo decomposition where the quinone becomes inactive.

Work is under progress where $Co(bpy)_3^{3+}$ is being attached to quinone, to create PTZ–Ru^{2+}–Q–Co, in which the electron hopefully is transferred the second step to $Co(bpy)_3^{3+}$. The $Co(bpy)_3^{3+}$ may then be substituted for potentially H_2-generating catalytic metal complexes.

Chapter 4

Mimicking the Light Harvesting Process – Artificial Antennas

An artificial antenna intended to mimic the light harvesting process in natural photosynthesis is usually constructed of several molecular components. Each component has its own special function in the energy transfer process, like absorption at different wavelengths, lowest excited state energy (energy trap), or just a bridge connecting two light absorbing components. If the excitation energy is going to be transferred between many components the rate of each energy transfer step will be very important. Efficient energy transfer over long distances, without large losses along the way, is important in molecular devices such as larger antenna systems [17] and molecular photonic wires [70].

In the first section in this chapter the spectroscopic properties of polynuclear transition metal complexes are presented, to give a background for the interpretation of the results obtained in paper V. Thereafter a summary of the results on ultra fast energy transfer between Ru(II) and Os(II) in a small artificial antenna fragment will be given, and this will be followed by some comments of the energy transfer mechanism.

4.1 Artificial antennas based on transition metal complexes

Professor Balzanis group in Bologna and professor Campagnas group in Messina have synthesized and studied dendrimers of different size, based on transition metal complexes [17]. The synthetic procedure allows a control of the exact position of each metal complex. The dendrimers are very interesting for several reasons. The ability to absorb light increases with the number of metal centers and multielectron reduction and oxidation can occur at certain potentials. The dendrimers also show efficient excitation energy transfer to the lowest excited state. To construct these large supramolecular complexes ruthenium and osmium have been used as metal centers, 2,3-dpp and 2,5-dpp as bridging ligands (dpp=bis(2-pyridyl)pyrazine), and bpy and biq (biq=2,2´-biquinoline) as terminal ligands.

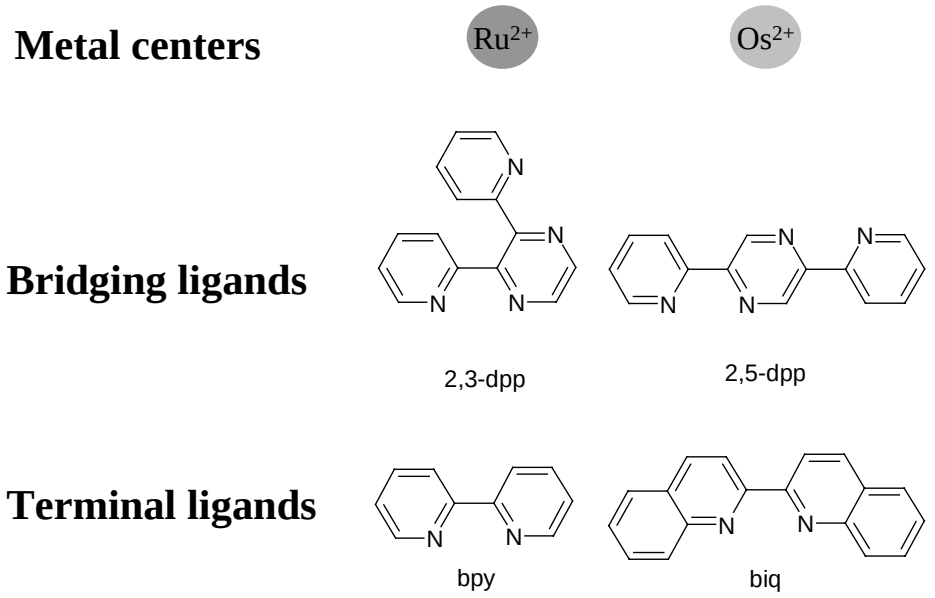

Figure 4.1 Structure of the bridging and terminal ligands.

The absorption spectrum of the polynuclear complexes show that the extinction coefficient increases with the number of metal centers that is incorporated in the structure. The absorption in the both the UV and visible spectral range can therefore be very large, with extinction coefficients of 1×10^5 $M^{-1}cm^{-1}$ for a complex with 22 metal centers [18,71]. Several overlapping absorption bands, corresponding to different MLCT transitions are contributing to the overall absorption. The energy of the transition depends on the metal and the ligand involved in the transition, and will largely be determined by the oxidation potential of the metal and the reduction potential of the ligand. The lowest excited state will be localized on the ligand easiest to reduce, i. e. with the best π-accepting ability. The energy of the lowest excited state of an osmium complex is lower than for the corresponding ruthenium complex. The energy ordering of the MLCT transitions involving Ru(II) and Os(II) as metal centers and the ligands in Figure 4.1 is [19]:

Os $\rightarrow$ μ-2,5-dpp < Os $\rightarrow$ μ-2,3-dpp < Os $\rightarrow$ biq < Ru $\rightarrow$ 2,5-dpp < Ru $\rightarrow$ 2,3-dpp < Os $\rightarrow$ bpy < Ru $\rightarrow$ bpy

The first reduction and first oxidation is ligand centered and metal centered respectively and follows the same pattern as the MLCT transitions. The 2,5-dpp ligand is easiest to reduce while bpy is most difficult to reduce, and Os(II) is oxidized at less positive potentials than Ru(II).

From redox data it is shown that the interaction between nearby units is noticeable for metals coordinated to the same ligand and for ligands coordinated to the same metal but direct interaction between units further apart is not detectable [72]. Therefore, neighboring ligands coordinated to the same metal but not directly involved in the transition also affects the energy of the MLCT transition through their electron donor ability. This will for example make the energy for $Ru(2,3\text{-dpp})_3^{2+}$ higher than for $Ru(2,3\text{-dpp})(bpy)_2^{2+}$. The electron donor ability increases in the series [72]:

$\mu\text{-}2,5\text{-dpp} \leq \mu\text{-}2,3\text{-dpp} < biq < bpy$

By varying the metal and the ligands it has been possible to construct complexes where efficient energy transfer occurs to the lowest excited state in pre-determined patterns. This has been obtained for complexes with four [73], six [74], ten [19], and 22 [71], metal centers. Energy transfer from the periphery to the center and from the center to the periphery has been obtained in some of the complexes. In larger structures a unidirectional energy transfer will require an increased number of metals and ligands to accomplish enough variation of excited state energies. Electron donating or accepting substituents on the peripheral ligands can also be used to alter the energy of the excited states in the periphery and thereby creating a gradient for energy transfer.

Efficient energy transfer to the metal unit with the lowest excited state energy has earlier been demonstrated by steady state emission measurements. It has been shown that irrespective of excitation wavelength the emission originates from the component with lowest excited state energy [75]. The assignment of the emission to certain components is based on comparisons with model compounds. For example in a binuclear complex $[(bpy)_2Ru^{II}(2,3\text{-dpp})Os^{II}(bpy)_2]^{4+}$, the ruthenium based emission is expected to occur at a wavelength comparable to the emission from ruthenium in the model compound $[(bpy)_2Ru^{II}(2,3\text{-dpp})Ru^{II}(bpy)_2]^{4+}$, and the osmium based emission is expected to occur at wavelengths comparable to the emission from $[(bpy)_2Os^{II}(2,3\text{-dpp})Os^{II}(bpy)_2]^{4+}$. In the heteronuclear compound only emission at wavelengths corresponding to the osmium based emission was detected, suggesting that the energy transfer from ruthenium to osmium was much faster than the spontaneous decay to the ground state ($\tau \approx 100$ ns for the Ru(II)-complexes).

To investigate the rate of energy transfer between two individual metal centers, two dinuclear Ru-Os complexes and the corresponding homometallic model complexes were selected. Except of being of fundamental interest the actual rate

of energy transfer between the individual units in a large complex intended to mimic the light harvesting process is of interest for the overall efficiency.

4.2 Ultra fast energy transfer between Ru(II) and Os(II) in a small artificial antenna

To study the energy transfer process in the Ru(II)-Os(II) complexes (Figure 4.2) transient absorption spectroscopy was chosen. The reason for this is the low radiative rate constant for these complexes. The ground state absorption spectra of the complexes are shown in Figure 4.3 and 4.4. The absorption bands corresponding to the MLCT transitions in the complexes appear at different energies in the spectrum.

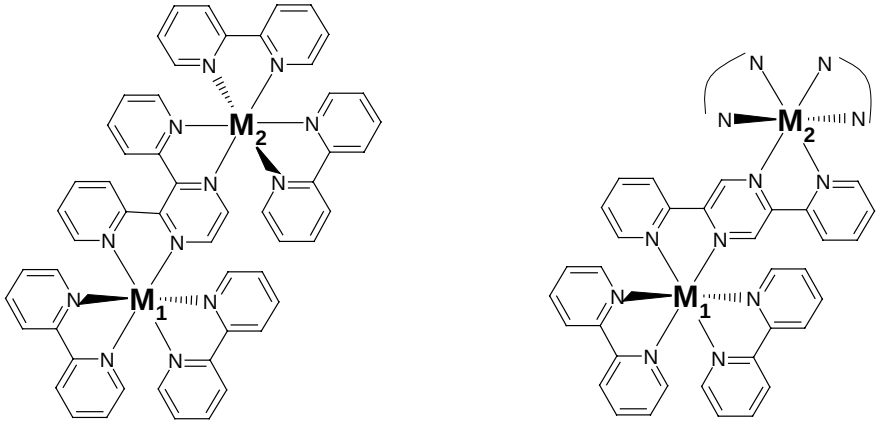

Ru^Ru	M_1=Ru, M_2=Ru	**Ru–Ru**	M_1=Ru, M_2=Ru, NN=bpy
Ru^Os	M_1=Ru, M_2=Os	**Ru–Os**	M_1=Ru, M_2=Os, NN=biq
Os^Os	M_1=Os, M_2=Os		

Figure 4.2 Structure of the binuclear complexes. Metal complexes with 2,3-dpp as bridging ligand (right) and metal complexes with 2,5-dpp as bridging ligand (left).

The difference between the absorption spectra of the complexes with the same bridging and peripheral ligands will depend on the metal centers. A redshift is observed when Ru(II) is replaced by Os(II). Another interesting feature in the absorption spectrum is the absorption extending to the red part for the osmium containing compounds. Due to the enhanced mixing of the singlet and triplet states by osmium, the probability of absorption from the singlet ground state to the lowest excited triplet states is slightly allowed and visible in the

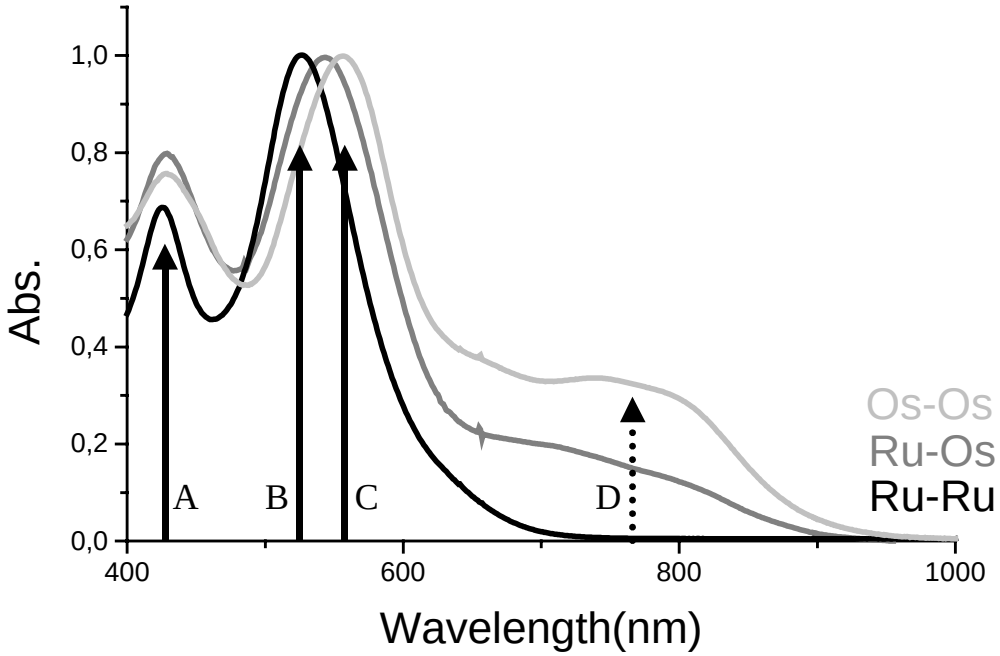

Figure 4.3 Absorption spectrum for the binuclear complexes with 2,3-dpp as bridging ligand, **Ru∧Ru** (black), **Ru∧Os** (dark gray) and **Os∧Os** (light gray). The different MLCT transitions indicated with arrows. RU→by and Os→by MLCT transitions at 425 NM (A), RU→2,3-dpp MLCT at 530 NM (B), Os→2,3-dpp MLCT at 556 NM (C) and the absorption to the ^{3}MLCT states of Os at 770 NM (D).

absorption spectrum. This allows direct observation of a bleaching that is unique for the osmium excited state at wavelengths where Ru(II) has no absorption in the ground state.

In the ruthenium-osmium complexes, the lowest excited state are the triplet states of osmium, and from the results obtained earlier in the steady state emission measurements the excitation energy is expected to be transferred to those states irrespective of excitation wavelength. Because of the overlapping absorption bands in the spectrum, selective excitation of one metal center is impossible, but even a 50 % selection of the MLCT transitions of ruthenium should be observable in the measurements when energy transfer occur with 100% efficiency to the osmium moiety. This would results in a shift of the excited state spectrum characteristic of ruthenium and osmium to a spectrum characteristic of only osmium.

The above expectations require that the excited state can be considered as localized to one metal center at a time. The distance between the metal centers

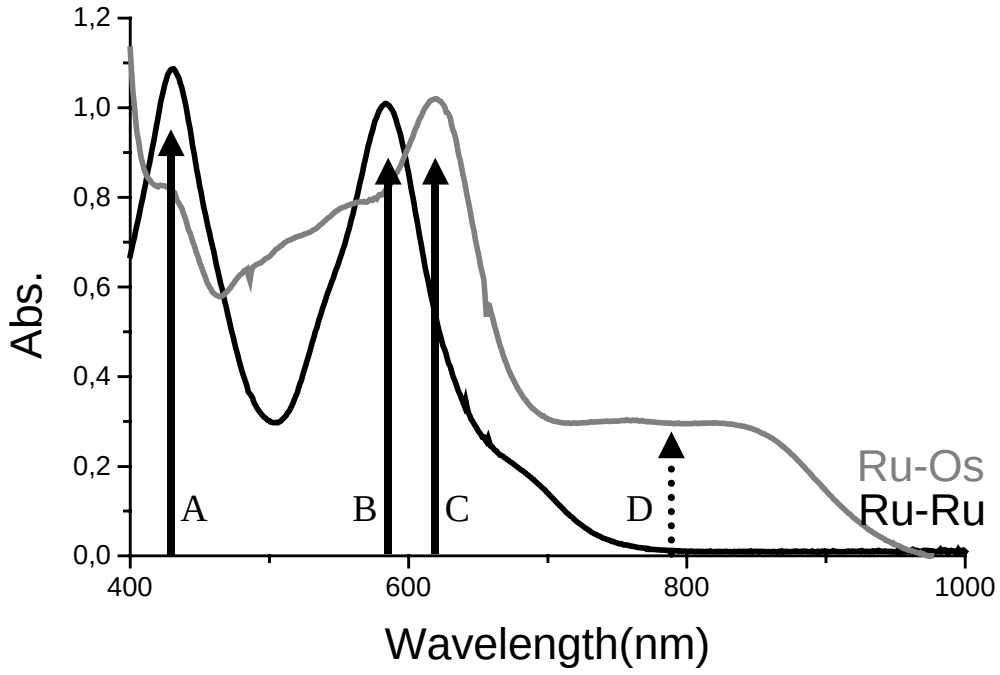

Figure 4.4 Absorption spectrum for the binuclear complexes with 2,5-dpp as bridging ligand, **Ru-Ru** (black) and **Ru-Os** (dark gray). The different MLCT transitions indicated with arrows. Ru→bpy at 430 nm (A), Ru→2,5-dpp at 580 nm (B), Os→2,5-dpp/biq at 625 nm (C) and the absorption to the ^{3}MLCT states of Os at 770 nm (D).

in these compounds is approximately 7-8 Å and the coupling is strong enough to allow very fast energy transfer to the metal unit with the lowest excited state energy. However the excited state is believed to be localized to one metal center at a time based on the following arguments.

The luminescence data has shown that the emission from the Ru(II)-Os(II) complexes agrees well with the emission from the lowest ^{3}MLCT states of osmium (based on studies on model compounds, Ru-Ru and Os-Os). The difference of the excited state energies is relatively large 0.2-0.4 eV, and the redox data shows that oxidation of the metal centers occur at different potentials characteristic of ruthenium and osmium respectively (1.25 V and 1.55 V) [76]. In the transient absorption measurements the bleaching of the Ru→bpy band is missing when energy transfer is completed. If the excited state was delocalized over both metal centers this band should be bleached.

Further support was obtained in an experiment where **Ru-Os**, was titrated with the oxidant Ce(IV) and the absorption spectrum measured at each added concentration. When Ce(IV) was added to oxidize osmium a NIR band

attributed to Ru(II)→Os(III) MMCT appeared. It was also initially a decrease in the intensity of the bands attributed to transitions to the lowest triplet and singlet MLCT states of the Os-moiety, at ≈800 and 625 nm, respectively. In contrast, the band at 575 nm attributed to the Ru→2,5-dpp transition (in analogy with the model complex) was not affected. This shows that the transitions observed are localized on one or the other metal unit. When more Ce(IV) was added, so that also the Ru(II) was oxidized, the Ru(II) bands disappeared, as well as the MMCT NIR band.

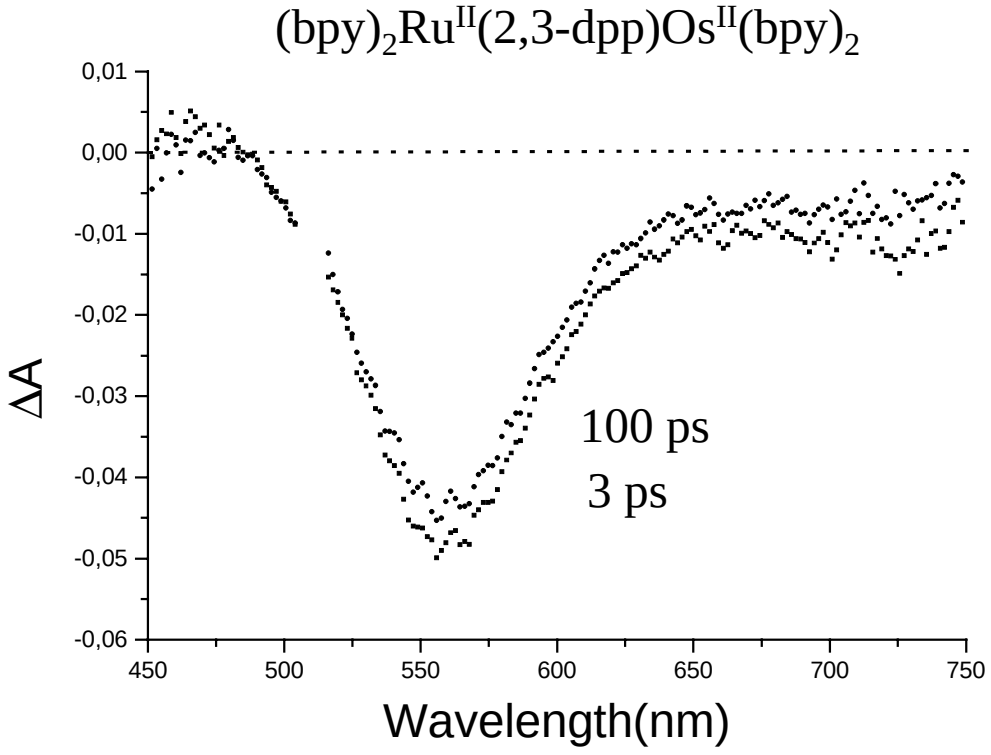

Figure 4.5 Transient absorption spectrum for **Ru∧Os** after excitation at 520 nm. The maximum of the bleaching agrees well with the maximum of the absorption band corresponding to the Os→2,3-dpp MLCT transition (556 nm).

After excitation of **Ru∧Os** (Figure 4.5) and **Ru-Os** (Figure 4.6) on the blue side of the lowest energy bands, the transient absorption spectra was for both complexes characteristic of the Os-moiety already after 3 and 5 ps respectively. No further shift of the spectrum was seen at longer time scales, just decay of the excited state of osmium ($\tau \approx 1$ ns). For **Ru∧Os** the maximum of the bleaching agreed well with the maximum of the absorption band corresponding to the Os→2,3-dpp MLCT transition (556 nm) in **Os∧Os** (Figure 4.3). For **Ru-Os** the maximum of the bleaching was at 625 nm, which is the maximum of the overlapping Os→2,5-dpp and Os→biq transitions. In addition, the bleaching of the Ru→bpy transition at 450 nm could not be observed.

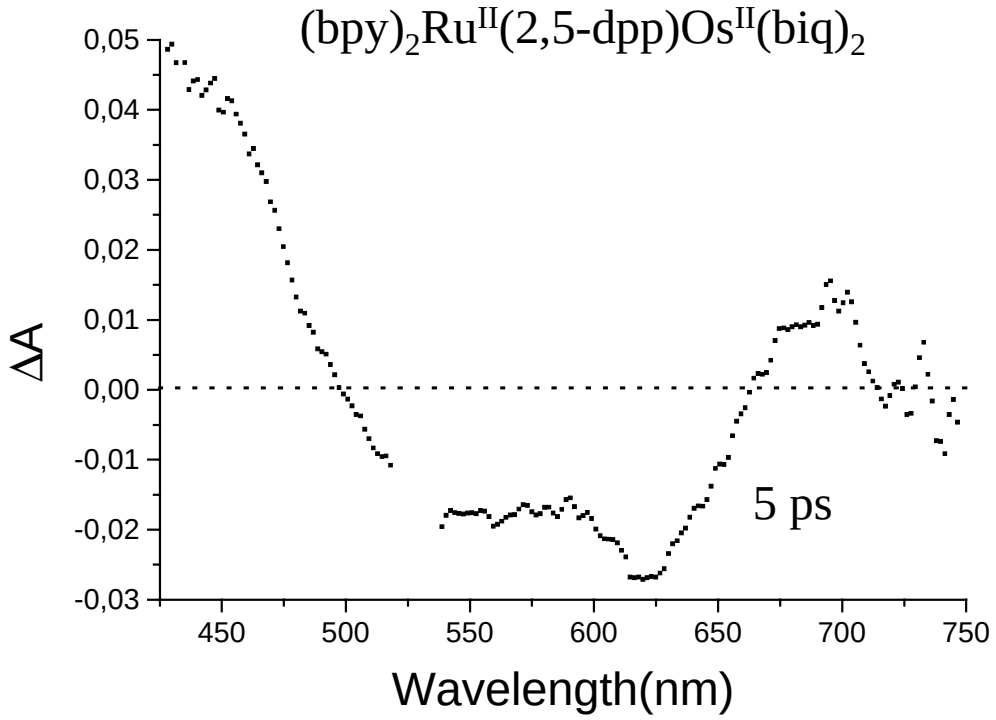

Figure 4.6 Transient absorption spectrum for Ru-Os after excitation at 528 nm. The bleaching at 625 nm agrees well with the absorption band corresponding to the Os→2,5-dpp/biq transition. The bleaching of the Ru→bpy band is not observed at 450 nm instead an absorption have appeared that probably can be assigned to transitions of the reduced 2,5-dpp [77] or biq [78] of the lowest Os-based MLCT state.

To investigate a possible spectral shift on shorter time scale. Kinetic traces were recorded at different wavelengths in the spectrum. Both for **Ru∧Os** and **Ru-Os** the results indicated that the energy transfer process occurred faster than the time resolution, $\tau<200$ fs. A spectral shift was obtained for **Ru∧Os** with a time constant of ≈400 fs, however kinetic traces for the model complexes **Ru∧Ru** and **Os∧Os**, showed the same behavior where energy transfer was not expected to give a spectral shift. The observed spectral shift in **Ru∧Os** was therefore not assigned to energy transfer between the metal centers. For further support of these findings, the polarization dependence of the pump-probe kinetic traces was investigated for **Ru∧Os**. With the bent 2,3-dpp as bridging ligand, energy transfer from one metal center to the other would change the direction of the transition dipole for the lowest MLCT state, that is believed to be directed along the metal-ligand axis [24]. This would result in a difference in the kinetic traces when the probe light is perpendicular or parallel to excitation. However the kinetic traces did not show a polarization dependence on a < 10 ps timescale, giving further evidence that the energy transfer in **Ru∧Os** was faster than the time resolution. The observed spectral shift with $\tau\approx400$ fs was instead attributed

to solvent and vibrational relaxation. A similar relaxation time has been reported for the mononuclear $Ru(bpy)_3^{2+}$ [27]. On longer timescale a slower polarisation decay was observed, attributed to molecular rotation.

The kinetic traces for **Ru-Os** indicated that the transient spectral features were characteristic of the excited osmium-moiety at all wavelengths also on a timescale <5 ps. No changes with time were detected except at 770 nm where a small increase of the bleaching was observed, with a time constant of $\tau \approx 800$ fs. A bleaching of the ground state absorption of the triplet MLCT states of osmium is expected at 700-800 nm after energy transfer to the osmium-moiety, since the model complex **Ru-Ru** has no ground state absorption at these wavelengths. However the amplitude of the ≈800 fs component is too small to account for EnT from an initial <50% population of Ru-based excited states. Moreover no spectral changes were found at any other wavelength, not even at the maximum of the Os→2,5-dpp/biq bleach (625 nm).

The conclusion was that also in the **Ru-Os** complex energy transfer occurred faster than the time resolution. Instead we attribute the observed dynamics at 770 nm ($\tau \approx 800$ fs), to vibrational and solvent relaxation also for this complex. When excitation was performed with 800 nm instead, there was no 800 fs component in the bleach, presumably because the excited state was populated close to the minimum of the potential energy surface.

4.3 Comments on a possible energy transfer mechanism

Energy transfer in Ru(II)-Os(II) complexes is usually assumed to occur via the Dexter mechanism due to the spin forbidden nature of the transitions involved [42]. However the Förster mechanism cannot be excluded due to the partial singlet character of the lowest excited states of ruthenium and osmium caused by the enhanced spin orbit coupling. Both mechanisms can act in parallel, but the relative contribution by the Förster mechanism might be low in ruthenium-osmium complexes due to the small radiative rate constant and low value of the overlap integral of the donor emission and acceptor absorption spectrum. The rate constant according to the Förster theory can be calculated from spectroscopic properties [39] and compared with the experimentally obtained rate constant. This is usually used as a way to estimate the relative contribution by the Förster mechanism. For the binuclear Ru(II)-Os(II) complexes investigated in paper V a Förster distance of 2 Å would be required to account for the rapid energy transfer process (based on comparison with similar Ru-Os complexes) and since the MLCT transitions are not very strong for these complexes, not even for the singlet-singlet transitions energy transfer via the

Förster mechanism seems unreasonable. If the Dexter mechanism is believed to be the dominant one, this is described as a double electron exchange and the rate constant can in the non adiabatic limit be expressed according to the expression for electron transfer in eq. 12 as described in chapter 2. Energy transfer from ruthenium to osmium occurred faster than the time resolution, $\tau<200$ fs. It seems therefore that the excited state dynamics of ruthenium [27,30] and the energy transfer between ruthenium and osmium in the investigated complexes occur on comparable time scales. The usual treatment applied for exchange energy transfer is valid for thermally relaxed states, and this is no longer true for the ultra fast energy transfer obtained in the present investigation.

When the excitation energy is going to be transferred several steps, in photonic wires or large antenna structures, the rate of each energy transfer step compared to the intrinsic decay rate of each metal unit will be important for the overall efficiency. In absence of osmium, the lifetime of the ruthenium-unit in **Ru∧Os** and **Ru-Os** is ≈100 ns, and if the energy transfer occurs faster than 200 fs, this means that 99.9998 % of the energy is transferred to the osmium-unit. If the energy transfer is assumed to occur with the same efficiency in each step the excitation energy can be transferred over long distances before any substantial losses of excitation. The investigated dinuclear ruthenium-osmium complexes are therefore very useful for construction of large and efficient artificial antennas. The remaining excitation energy can then eventually be used in a charge separation process in an artificial reaction center.

Appendix

Experimental

A.1 Femtosecond pump-probe measurements

The laser system used in the femtosecond transient absorption measurements is schematically shown in Figure A.1. It consists of two sub-systems that can operate at the same time, one system (Coherent) that generates femtosecond laser pulses at a frequency of 200 kHz and one system (Quantronix) that generates femtosecond laser pulses at a frequency of 1 kHz. For the experiments performed in this thesis, only the system operating at 1 kHz have been used.

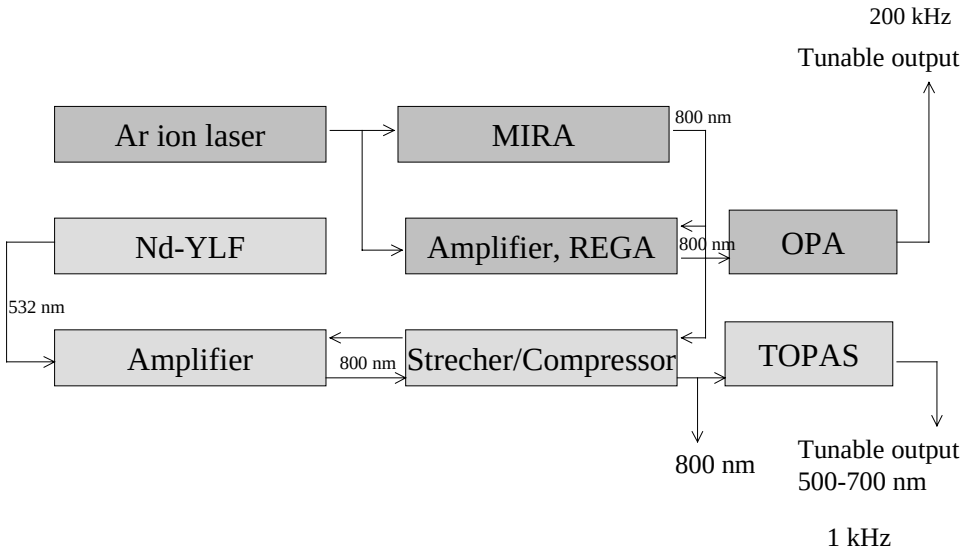

Figure A.1 Experimental setup.

The Ar-ion CW laser is pumping the mode-locked Ti-saphire laser (MIRA) generating laser pulses of 80 fs duration at about 800 nm (bandwidth ≈11 nm). The 800 nm laser pulses are then amplified by either the 200 kHz system or the 1 kHz system. In the 1 kHz system, a Q-switched Nd-YLF laser generating frequency doubled nanosecond laser pulses is pumping the Ti-sapphire amplifier laser. The mode-locked pulses from the Ti-sapphire laser (MIRA) are stretched in the Stretcher/Compressor and after stretching, these pulses are used to seed the amplifier. After amplification the output from the amplifier is compressed and characteristically, the pulses have an autocorrelation halfwidth of 190-200 fs and pulse energy of about 700 μJ

In the pump-probe measurements with the present setup (Figure A.1) the laser beam is split into two parts by a beam splitter. 70 % is passed trough an optical parametric amplifier (TOPAS) which generates visible light tunable between

500 and 700 nm. The output from the TOPAS is used for excitation i. e. to pump the sample. The pump light is passed through a chopper operating at a frequency between 75-110 Hz before it is focused and overlapped with the probe light in the sample.

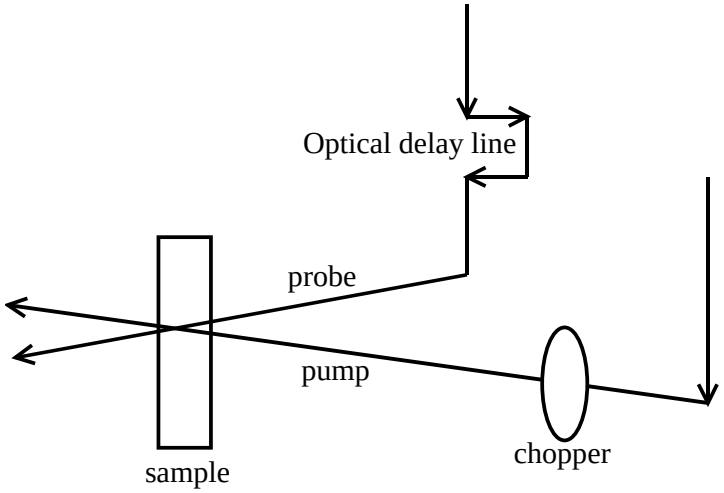

Figure A.2 Schematic picture of a pump probe experiment.

The remaining 30 % of the 800 nm is used for probing. To generate white light the beam is focussed in a sapphire window or CaF_2 (in some measurements water), the white light is then passed through an optical delay line before it is focused and overlapped with the pump light in the sample cell (1×10 mm). In the kinetic measurements the detection wavelengths are selected by a monochromator and then detected by a photomultiplier.

The timescale in the pump probe measurements is obtained by varying the time delay between the pump and probe. This is accomplished by moving the mirror of the optical delay line in small steps. In the present setup we have the ability to use two different delay lines, one that gives a total time window of 1 ns for detection and one that gives a 5 ns time window. In paper V only the short delay line have been used, whereas a time window of 5 ns have been necessary for some of the traces in paper IV. The alignment of the delay line is of crucial importance in a pump probe experiment. If the beam is not parallel when entering and exiting the reflecting mirror the overlap with the pump will change when the mirror is moved. To minimize this effect, the delay line is aligned by observing the beam at far field. When using the long delay line, kinetic traces of the bleaching $Ru(bpy)_3^{2+}$ was usually measured on a long timescale (50-5000 ps) as a reference. The lowest ^{3}MLCT state of $Ru(bpy)_3^{2+}$ is not expected to decay significantly on the 5 ns timescale, and the observed trace should not show any changes. On much shorter timescales, as for the investigation of the energy

transfer process in the ruthenium-osmium complexes, only the solvent (acetonitrile) was measured to exclude that the observed dynamics originated from intrinsic effects of the solvent.

In the polarization dependent measurements, a polarizer was positioned in the pump beam and in the probe beam respectively. A $\lambda_{1/2}$ plate was positioned before the white light generation in the probe beam to rotate the fundamental laser light 50 °. The polarizer in the probe beam was adjusted to select either the direction parallel or perpendicular to excitation.

The detection of the absorbance change upon excitation is performed with the Lock-In Amplifier technique. Variations of the probe light which have the same frequency as the chopper are registrated and the difference between the white light intensity with and without excitation ($I–I_0$), is obtained. Since the signal changes are small to the changes in absorption, i.e: $(I–I_0)/I_0 << 1$, they are proportional. A disadvantage is however that the absolute value of the delta absorption cannot be given since $\Delta A = –\lg (I/I_0)$.

In the spectral measurements a spectrograph (MS 257, Oriel instruments) equipped with a CCD-detector was used. Instead of a chopper a shutter is placed in the pump beam, the intensity of the white light is measured with and without excitation and ΔA is obtained. If spectra are taken at short time delays, corrections have to be made for the group velocity dispersion. In the femtosecond measurements presented in this thesis this have not been done since only kinetic traces have been used to interpret the results on shorter time scales.

A.2 Nanosecond flash photolysis measurements

In the flash photolysis experiments mainly two different laser systems have been used. A commercial system from Applied Photophysics, where a Nd-YAG laser (Spectron Laser system) generating laser pulses of 7 ns duration at 532 nm was used for excitation. The analysing light was provided from a pulsed xenon lamp, and the different detection wavelengths were selected with a monochromator connected to a R 928 photomultiplier. The signal from the photomultiplier was transferred to a digital oscilloscope.
In the other system, an ELI-94 excimer laser operating with XeCl at 308 nm was used to pump a dye laser (LT-1113). The output from the dye laser used for excitation, gave laser pulses at 460 nm with 20 ns duration. The analysing light was provided by a pulsed xenon lamp and for detection a photomultiplier coupled to a digitizer (Techtronix) was used.

Acknowledgements

First of all I would like to thank my supervisor *Leif Hammarström*, for your knowledge, patience and your ability to inspire when everything seems hopeless.

Mats Almgren my supervisor during the first year for support and for creating such a nice and friendly working atmosphere.
Jan Davidsson for teaching me how to handle the femtosecond laser system and for always finding time to help.
All present and previous members of *The Consortium for Artificial Photosynthesis* are thanked for nice cooperation.
All colleagues and friends at the Department of Physical Chemistry especially *Margit*, *Laila*, *Gösta*, and *Sven* for always being very helpful.

Malin för trevligt samarbete, roliga konferenser, och för ditt glada och trevliga sätt.
Mikael; Vi har slitit tillsammans och under tiden har våra diskussioner och roliga upptåg i lasergrottan förgyllt tillvaron.

Maria för att du är en god vän. Våra långa telefonsamtal, många gympapass och trevliga luncher har varit ett stöd och en inspirationskälla.

Min familj

Mormor *Judith* och farmor *Karin* samt *Allan*, *Gunnar* och *Elisabet* för att ni alltid har brytt er om och funnits där.

Mamma och *Tomas* för stöd och uppmuntran.

Micael, *Jonas* och *Linn*: Det som verkligen gör mig lycklig är att se era glada ansikten.

Bibliography

[1] a) Deisenhofer, J.; Norris, J. R. *In the Photosynthetic Reaction Center*, Academic press: San Diego, 1993, Vol 1-2. b) *Oxygenic Photosynthesis: The Light Reactions*, ed D. R. Ort and C. F. Yocum, Kluwer Academic Publishers, Dordrecht, The Netherlands, 1996.

[2] Sundström, V.; Pullerits, T.; van Grondelle, R. *J. Phys. Chem. B* **1999**, 103, 2327.

[3] a) Yachandra, V. K.; Sauer, K.; Klein, M. P. *Chem. Rev.* **1996**, 96, 2927. b) Ruettinger, W.; Dismukes, G. C. *Chem Rev.* **1997**, 97, 1.

[4] Hoganson, C. W.; Babcock, G. T. *Science* **1997**, 277, 1953.

[5] Tommos, C.; Babcock, G. T. *Acc. Chem. Res.* **1998**, 31, 18.

[6] Limburg, J.; Vrettos, J. S.; Liable.Sands, L. M.; Rheingold, A. L.; Crabtree, R. H.; Brudwig, G. W. *Science,* **1999**, 283, 1524.

[7] Wasielewski, M. R. *Chem. Rev.* **1992**, 92, 435.

[8] Sauvage, J.-P.; Collin, J.-P.; Chambron, J.-C.; Guillerez, S.; Coudret, C.; Balzani, V.; Barigelletti, F.; De Cola, L.; Flamigni, L. *Chem. Rev.* **1994**, 94, 993.

[9] Gust, D.; Moore, T. A.; Moore, A. L. *Acc. Chem. Res.* **1993**, 26, 198.

[10] Kurreck, H.;Huber, M. *Angew. Chem. Int. Ed. Engl.* **1995**, 34, 849.

[11] Imahori, H.; Sakata, Y. *Eur. J. Org. Chem.* **1999**, 2445.

[12] Molnar, S.; Nallas, G.; Bridgewater, J.; Brewer, K. *J. Am. Chem. Soc.* **1994**, 116, 5206.

[13] a) Steinberg-Yfrach, G.; Liddell, P. A.;Hung, S.-C.; Moore, A. L.; Gust, D.; Moore, T. A. *Nature*, **1997**, 385, 239-241. b) Steinberg-Yfrach, G.;Rigaud, J.-L.; Durantini, E. N.; Moore, A. L.; Gust, D.; Moore, T. A. *Nature*, **1998**, 392, 479.

[14] Hsiao, J.-S.; Krueger, B. P.; Wagner, R. W.; Johnson, T. E.; Delaney, J. K.; Mauzerall, D. C.; Fleming, G. F.; Lindsey, J. S.; Bocian, D. F.; Donohoe, R. J. *J. Am. Chem. Soc.* **1996**, 118, 11181-11193.

[15] Lin, V. S.-Y.; DiMagnio, S. G.; Therien, M. J.; *Science*, **1994**,1105.

[16] Kuciauskas, D.; Liddell, P.A.; Lin, S.; Johnson; T. E.; Weghorn, S. J.; Lindsey, J. S.; Moore, A. L.; Moore, T. A.; Gust, D. *J. Am. Chem. Soc.* **1999**, 121, 8604.

[17] Balzani, V.; Campagna, S.; Denti, G.; Juris, A.; Serroni, S.; Venturi, M. *Acc. Chem. Res.* **1998**, 31, 26-34 (and references therein).

[18] Campagna, S.; Denti, G.; Serroni, S.; Juris, A.; Venturi, M.; Ricevuto, V.; Balzani, V. *Chem. Eur. J.* **1995**, 1, 211.

[19] Denti, G.; Campagna, S.; Serroni, S.; Ciano, M.; Balzani, V.; *J. Am. Chem. Soc.* **1992**, 114, 2944-2950.

[20] Juris, A.; Balzani, V.; Barigelletti, F.; Campagna, S.; Belser, P.; von Zelewsky, A. *Coord. Chem. Rev.* **1988**, 84, 85.
[21] Kalyanasundaram, K. In *Photochemistry of Polypyridine and Porphyrin Complexes*; Academis Press: London, 1992.
[22] De Armond , M. K.; Myrick, M. L. *Acc. Chem. Res.* **1989**, 22, 364.
[23] Meyer, T. J. *Pure and Appl. Chem*. **1986**, 58, 1193.
[24] Myrick, M. L.; Blakley, R. L.; DeArmond, M. K.; Arthur, M. L. *J. Am. Chem. Soc.* **1988**, 110, 1325.
[25] Cooley, L. F.; Bergquist, P.; Kelley, D. F. *J. Am. Chem. Soc*. **1990**, 112, 2612.
[26] Malone, R. A.; Kelley, D. F. *J. Chem. Phys.* **1991**, 95, 8970.
[27] Yeh, A. T.; Shank, C. V.; McCusker, J. K. *Science*, **2000**, 289, 935.
[28] Hager, G. D.; Crosby, G. A.; *J. Am. Chem. Soc.* **1975**, 97, 7031
[29] Kober, E. M.; Meyer, T. J. *Inorg. Chem.* **1984**, 23, 3877.
[30] Damrauer, N. H.; Cerullo, G.; Yeh, A.; Boussie, T. R.; Shank, C. V.; McCusker, J. K. *Science*, **1997**, 275, 54.
[31] Demas, J. N.; Crosby, G. A. *J. Am. Chem. Soc.* **1971**, 93, 2841.
[32] Caspar, J. V.; Kober, E. M.; Sullivan, B. P. Meyer, T. J. *J. Am. Chem. Soc.* **1982**, 104, 630.
[33] Gorelsky, S. I.; Dodsworth, E. S.; Lever, A. B. P.; Vlcek, A. A. *Coord. Chem. Rev.* **1998**, 174, 469, and references therein.
[34] Sutin, N. *Acc. Chem. Res.* **1982**, 15, 275-282.8[
[35] Murtaza, Z.; Graff, D. K.; Zipp, A. P.; Worl, L. A.; Jones; W. E.; Bates, W. D.; Meyer, T. J. *J. Phys. Chem.* **1994**, 98, 10504.
[36] McConnell, H. M. *J. Chem. Phys.* **1961**, 35, 508.
[37] Jortner, J. *J. Chem. Phys.* **1976**, 64, 4860.
[38] Marcus, R. A.; Sutin, N. *Biochim. Biophys. Acta* **1985**, 811, 265.
[39] Förster, Th. H. *Discuss. Faraday Soc.* **1959**, 27, 7.
[40] Van Der Meer, B. W.; Coker, G.; Simon Chen; S.-Y. In *Resonance Energy Transfer*, VCH Publishers Inc., New York, 1994.
[41] Dexter, D. L. *J. Chem. Phys.* **1953**, 21, 836.
[42] De Cola, L.; Belser, P. Coord. Chem. Rev. 1998, 177, 301-346.
[43] Balzani, V.; Bolletta, F.; Scandola, F. *J. Am. Chem. Soc.* **1980**, 102, 2152.
[44] Scandola, F.; Balzani, V. *J. Chem. Educ*. **1983**, 60, 814.
[45] Sun, L.; Hammarström, L.; Norrby, T.; Berglund, H.; Davydov, R.; Andersson, M.; Börje, A.; Korall, P.; Philouze, C.; Almgren, M.; styring, S.; Åkermark, B. *J. Chem. Soc. Chem. Commun.* **1997**, 607.
[46] Sun, L.; Berglund, H.; Davydov, R.; Norrby, T.; Hammarström, L.; Korall, P.; Börje, A.; Philouze, C.; berg, K.; Tran, A.; Andersson, M.; Stenhagen, G.; Mårtensoon, J.; Almgren, M.; Styring, S.; Åkermark, B. *J. Am. Chem. Soc.* **1997**, 119, 6996.

[47] Magnuson, A.; Frapart, Y.; Abrahamsson, M.; Horner, O.; Åkermark, B.; Sun, L.; Girerd, J.-J.; Hammarström, L.; Styring, S. *J. Am. Chem. Soc.* **1999**, 121, 89-96.

[48] Sjödin, M.; Styring, S.; Sun, L.; Åkermark, B.; Hammarström, L.; *J. Am. Chem. Soc.* **2000**, 122, 3932-3936.

[49] Berg, K. E.; Tran, A.; Raymond, M. K.; Abrahamsson, M.; Volny, J.; Redon, S.; Andersson, M.; Sun, L.; Styring, S.; Hammarström, L.; Toftlund, H.; Åkermark, B. Eur. J. *Inorg. Chem.* Accepted **2000**.

[50] Sun, L.; Raymond, M. K.; Magnuson, A.; LeGourriérec, D.; Tamm, M.; Abrahamsson, M.; Huang Kenéz, P.; Mårtensson J.; Stenhagen, G.; Hammarström, L.; Styring, S.; Åkermark, B. *J. Inorg. Biochem.* **2000**, 78, 15-22.

[51] Demas, J. N.; Addington, J. W. *J. Am. Chem. Soc.* **1976**, 98, 5800

[52] Gaines, G. L.; O´Neil, M. P.; Svec, W. A.; Niemczyk, M. P.; Wasielewski, M. R. *J. Am. Chem. Soc.* **1991**, 113, 719.

[53] Wasielewski, M. R.; Johnson, D. G.; Svec, W. A.; Kersey, K. M.; Minsek, D. W. J. Am. Chem. Soc. 1988, 110, 7219.

[54] Chen, P.; Meyer, T. J. *Inorg. Chem.* **1996**, 35, 5520.

[55] Bock, C. R.; Meyer, T. J.; Witten, D. G. *J. Am. Chem. Soc.* **1975**, 97, 2909.

[56] Serpone, N. In *Photoinduced Electron Transfer*; Fox, M. A., Chanon, M., Eds.; Elsevier: Amsterdam, 1988; Vol. Part D, p 47.

[57] Darwent, J. R.; Kalyanasundaram, K. *J. Chem. Soc. Faraday Trans.* **1981**, 77, 373.

[58] Land, E. J.; Prütz, W. A. *Int. J. Radiat. Biol.* **1979**, 36, 75.

[59] Babcock, G. T.; Sauer, K. *Biochim. Biophys. Acta* **1975**, 376, 315.

[60] Barry, B. A.; Babcock, G. T. *Chem. Scr.* **1988**, 28 A, 117.

[61] Burdinski, D.; Wieghardt, K.; Steenken, S.; *J. Am. Chem. Soc.* **1999**, 121, 10781.

[62] Burdinski, D.; Bothe, E.; Wieghardt, K. *Inorg. Chem.* **2000**, 39 105.

[63] Sun, L.; Hammarström, L.; Åkermark, B.; Styring, S. *Chem. Soc. Rev.* **2001**, 30, 36-49.

[64] Yonemoto, E. H.; Riley, R. L.; Kim, Y.; Atherton, S. J.; Schmehl, R. H.; Mallouk, T. E. *J. Am. Chem. Soc.* **1992**, 114, 8081-8087.

[65] Goulle, V.; Harriman, A.; Lehn, J.-M. *J. Chem. Soc. Chem. Commun.* **1993**, 1034.

[66] Berkoff, R.; Krist, K; Gafney, H. D. *Inorg. Chem.* **1980**, 19, 1.

[67] Opperman, K. A.; Mecklenburg, S. L.; Meyer, T. J. *Inorg. Chem.* **1994**, 33, 5295-5301.

[68] Treadway, J. A.; Chen, P.; Rutherford, T. J.; Keene, F. R.; Meyer, T. J. *J. Phys. Chem.* **1997**, 101, 6824-6826.

[69] Larson, S. L.; Elliot, C. M.; Kelley, D. F. *J. Phys. Chem.* **1995**, 99, 6530.

[70] Schlicke, B.; De Cola, L.; Belser, P; Balzani, V. *Coord. Chem Rev.* **2000**, 208, 267.

[71] Serroni, S.; Juris, A.; Venturi, M.; Campagna, S.; Resino, I.; Denti, D.; Credi, A.; Balzani, V. *J.Mater. Chem.* **1997**, 7, 1227-1236.

[72] Denti, G.; Campagna, S.; Sabatino, L.; Serroni, S.; Ciano, M.; Balzani, V. *Inorg. Chem.* **1990**, 29, 4750-4758.

[73] Denti, G.; Serroni, S.; Campagna, S.; Ricevuto, V.; Balzani, V. *Inorg. Chim. Acta*. **1991**, 182, 127-129.

[74] Campagna, S.; Denti, G.; Serroni, S.; Ciano, M.; Balzani, V. *Inorg. Chem.* **1991**, 30, 3728-3732.

[75] Juris, A.; Balzani, V.; Campagna, S.; Denti, G.; Serronni, S.; Frei, G.; Güdel, H. *Inorg. Chem.* **1994**, 33, 1491-1496.

[76] Campagna, S.; Denti, G.; Sabatino, L.; Serroni, S.; Ciano, M.; Balzani, V. *J.Chem. Soc., Chem. Commun.* **1989**, 1500.

[77] Balzani, V. unpublished results

[78] Meyer, G. personal communication